2019

In situ formed magnetic ionic liquids: DNA extraction performance and fluorescence-compatibility in bioanalytical applications

Ashley Nicole Bowers
Iowa State University

In situ formed magnetic ionic liquids: DNA extraction performance and fluorescence-compatibility in bioanalytical applications

by

Ashley Nicole Bowers

A thesis submitted to the graduate faculty

in partial fulfillment of the requirements for the degree of

MASTER OF SCIENCE

Major: Analytical Chemistry

Program of Study Committee:
Jared L. Anderson, Major Professor
Robbyn K. Anand
Aaron J. Rossini
Emily A. Smith

The student author, whose presentation of the scholarship herein was approved by the program of study committee, is solely responsible for the content of this thesis. The Graduate College will ensure this thesis is globally accessible and will not permit alterations after a degree is conferred.

Iowa State University

Ames, Iowa

2019

TABLE OF CONTENTS

Page

ACKNOWLEDGMENTS

I would first like to thank my major professor, Dr. Jared Anderson, for giving me the opportunity to work in his laboratory during my graduate studies. I would also like to thank him for his guidance, expertise and teaching, as it has continually helped me grow as a chemist. He is a passionate and extraordinary scientist and I'm thankful for all that I've learned while being in his research group. I would also like to thank my committee members, Dr. Robbyn Anand, Dr. Emily Smith and Dr. Aaron Rossini for their guidance, support and time. I also thank Dr. Jacob W. Petrich for his helpful mentorship and collaboration throughout the course of this research. Also, thank you to Dr. María José Trujillo-Rodríguez, Dr. Kalyan Santra and Anthony Song for your support, sharing your knowledge and always being willing to help me.

I would like to thank all my current and former group members: Omprakash Nacham, Kevin Clark, Jiwoo An, Stephen Pierson, He Nan, Marcelino Varona, Miranda Emaus, Gabriel Odugbesi, Chenghui Zhu, Qamar Farooq, Han Chen, Philip Eor and Nabeel Abbasi, along with all visiting professors and postdoctoral researchers: Dr. Dongmei Lu, Dr. Kosuke Kuroda, Dr. Xi-Tian Peng, Dr. María José Trujillo-Rodríguez, Dr. Xiong Ding, Dr. Deepak Chand and Dr. Arianna Marengo for their support and help along the way. Also thank you to visiting graduate students: Israel Donizéti de Souza, Idaira Pacheco-Fernández, Jakub Šulc and Ester Peris García.

I sincerely thank my parents, Anna and Steve Bowers, and my sister, Lauren, for always encouraging me, every step of the way. Thank you for your great support throughout this challenging and life-changing experience. I appreciate you always being there for me.

Lastly, I would also like to thank my friends, colleagues, and the chemistry department faculty and staff at Iowa State University for their support.

ABSTRACT

Extracting genomic DNA from complex biological sample matrices is often the first step in numerous molecular biology procedures such as polymerase chain reaction (PCR), cloning, and gene therapy. Obtaining high yields and pure DNA presents a significant sample preparation challenge in nucleic acid analysis. Current methodologies such as the phenol-chloroform extraction use toxic organic solvents and commercially available kits are often very expensive and have limited reusability. Magnetic ionic liquids (MILs) have gained popularity as inexpensive, environmentally benign and tunable extraction solvents. MILs are a subclass of ionic liquids containing a paramagnetic component in the cation or anion, allowing them to be manipulated using an external magnetic field. This thesis describes the use of a new class of MILs featuring metal-containing cations for DNA extraction and their compatibility with fluorescence-based detection methods. Two studies were conducted to address this goal. The first study focused on the DNA extraction efficiency of a new class of MILs using *in situ* dispersive liquid-liquid microextraction (DLLME) versus conventional DLLME to assess the extraction of DNA sequences of varied sizes. Extraction efficiencies were obtained using indirect detection using anion-exchange high performance liquid chromatography with diode array detection and fluorescence spectroscopy. However, to minimize steps in the sample preparation process, it is useful to directly analyze the DNA within the enriched MIL microdroplet therefore, in a second study the fluorescence quenching effects of the MIL were evaluated. These studies provide an insight into how the paramagnetic metal (Ni, Co, Mn) and ligand used in the design of the MIL can be tailored in order to achieve highly efficient DNA extraction and the subsequent influence of the MIL on the fluorescence signal in downstream analysis.

CHAPTER 1. GENERAL INTRODUCTION

1.1. Brief Overview of DNA Extraction and Purification Methods

Deoxyribonucleic acid (DNA) is the genetic material found in all organisms [1]. DNA analysis is a critical component in numerous applications in medicine [2], forensics [3], molecular biology [4] and food safety [5]. Prior to DNA analysis, the extraction and purification of DNA from biological matrices must be performed. Obtaining high quality DNA is crucial for the success of downstream applications such as polymerase chain reaction (PCR) and fluorescence-based assays [6, 7]. Nucleic acid extraction and purification procedures are often lengthy and tedious; therefore, they have been considered a hindrance in the sample preparation workflow.

Traditional nucleic acid purification techniques include liquid-liquid extraction (LLE) and solid-phase extraction (SPE) [6]. The most commonly used LLE procedure uses phenol and chloroform, where, after cell lysis using heat or surfactants, DNA is extracted into the aqueous phase and the other cellular components (e.g., proteins and lipids) partition into the organic phase [6]. Although the phenol-chloroform extraction method can be used for a variety of sample matrices and large amounts of DNA can be obtained, it uses toxic organic solvents, involves multiple steps, and lacks selectivity. Many commercially available kits contain a solid-phase support such as silica, cellulose, magnetic particles, or an anion-exchange resin [6]. These kits can only be used a limited number of times, are very costly and may require specific equipment for use. Due to the aforementioned drawbacks of current LLE and SPE methods for nucleic acid extractions, the use of ionic liquids (ILs) and their magnetic counterparts, magnetic ionic liquids (MILs), in bioanalytical sample preparation methodologies has grown in recent years [8].

1.2. Introduction to Magnetic Ionic Liquids in DNA Extractions and Analysis

ILs are molten salts comprised entirely of ions with melting points at or below 100 ºC [9]. ILs possess many unique physiochemical properties such as relatively high thermal stability, low melting points, variable viscosity, broad electrochemical stability and unique solvation capabilities of both polar and non-polar compounds [9]. The incorporation of a paramagnetic component in the cation and/or anion of the IL structure has created a subclass of ILs called magnetic ionic liquids (MILs), which have magnetic properties. The cationic and/or anionic moieties of both ILs and MILs can be structurally tuned for specific applications and interactions with certain analytes, which has immensely popularized their use in analytical chemistry. Some common cations and anion structures of ILs and MILs are shown in Figure 1.1.

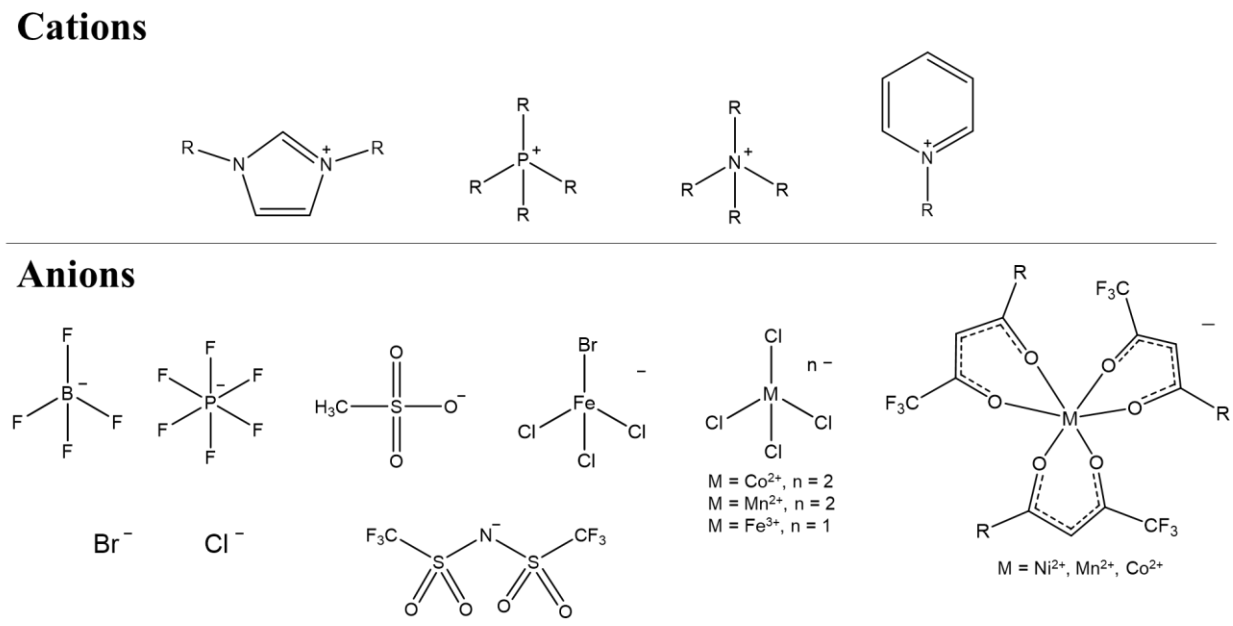

Figure 1.1. Common cations and anion structures used in ILs and MILs.

ILs and MILs have been used in a variety of microextraction procedures for the preconcentration of DNA such as single-drop microextraction (SDME), solid-phase

microextraction (SPME), and dispersive liquid-liquid microextraction (DLLME). In SDME, both direct immersion and headspace sampling methods can be used. In this technique, analytes partition from the aqueous phase or headspace into a microdroplet extraction phase suspended from a syringe needle or magnetic rod [10]. Due to the small surface area of the microdroplet, long extraction times are needed in SDME to achieve high extraction efficiencies [11, 12]. In SPME, a fiber is coated with an extraction material, such as a polymeric ionic liquid, which is reusable upon desorption of the extracted analytes [13]. However, the extraction and desorption processes can be lengthy, which decreases the overall sample throughput. The drawbacks of these methods have led to liquid-based extraction methods such as DLLME to be more favorable [8].

In conventional DLLME, a mixture of an extraction and dispersive solvent are added to an aqueous solution containing analytes [14]. Then, the solution is homogeneously mixed, generally by vortex, to promote dispersion of the microdroplets and enrichment of analytes from the sample matrix into the extraction phase. After the extraction is complete, centrifugation is typically performed to recover the extraction phase. Traditionally, hydrophobic ILs have been used as extraction solvents in DLLME, however recent reports using hydrophobic MILs have emerged, which allow for collection of the MIL extraction phase with a magnet, affording more efficient extraction methods [15]. In a modification of conventional DLLME called in situ DLLME, a hydrophilic IL, dispersive solvent and an anion-exchange reagent are added to the aqueous sample solution to generate a hydrophobic IL [9]. This metathesis reaction occurs during the extraction procedure, where numerous microdroplets of the extraction phase are dispersed throughout the sample solution, interacting with analytes. Higher extraction efficiencies are generally achieved with in situ DLLME than with conventional DLLME,

because the anion-exchange reaction increases the surface area of the extraction phase within the sample solution [16, 17]. A comparison of the conventional MIL-DLLME and in situ MIL-DLLME methods is shown in Figure 1.2.

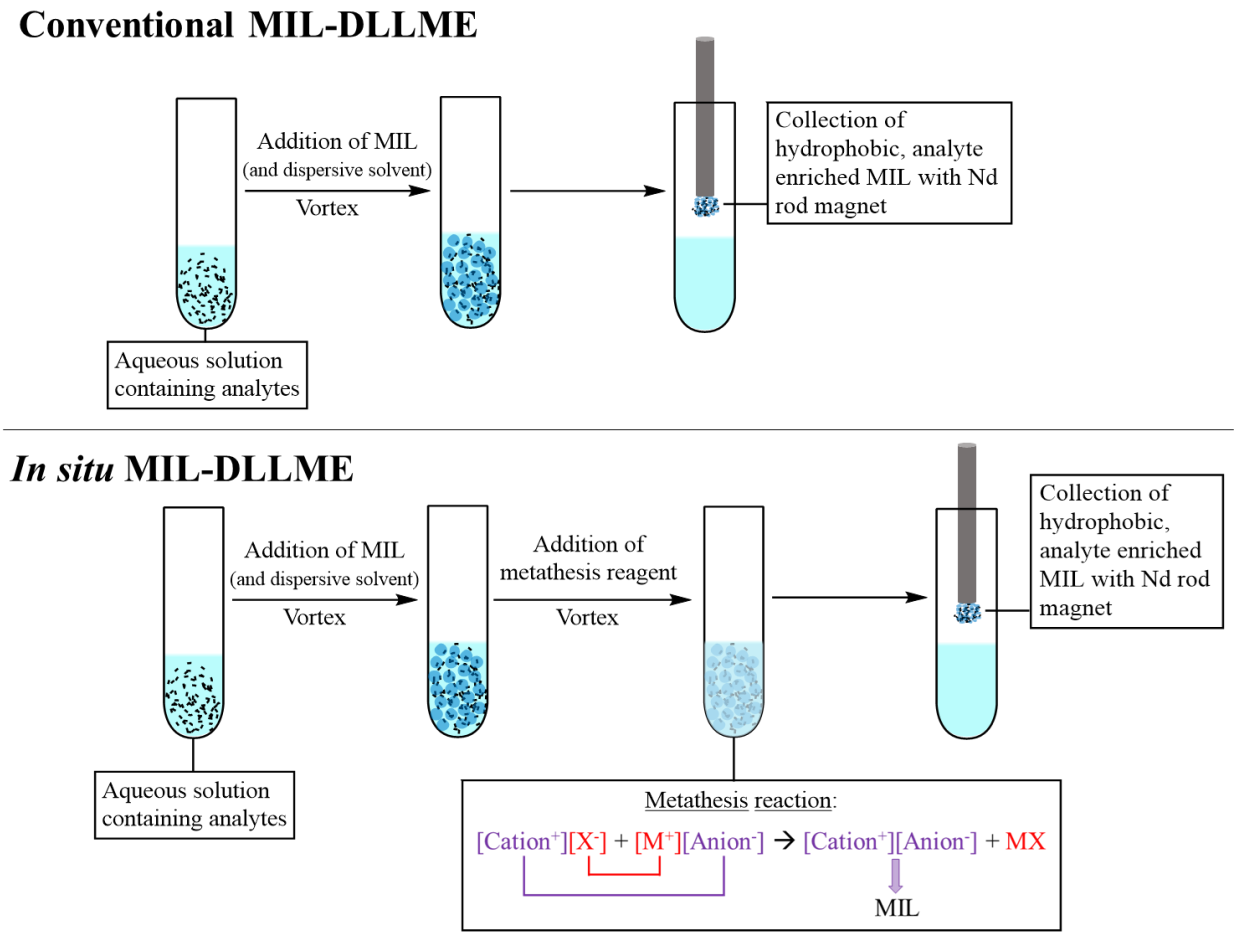

Figure 1.2. Schematic describing conventional MIL-DLLME and *in situ* MIL-DLLME methods.

MILs have been used for the extraction of DNA using conventional DLLME methods [11, 18, 19]. In these studies, the paramagnetic component of the MIL is within the anion. This restricts the use of these MILs in in situ DLLME because the paramagnetic anion would be exchanged during the metathesis reaction, thereby hindering magnetic collection of the MIL extraction phase. Recently, a new generation of MILs containing the paramagnetic component in

the cation and chloride anions were applied for the extraction of DNA using in situ DLLME [17]. During extraction, the water-soluble MIL reacts with the bis[(trifluoromethyl)sulfonyl]imide anion to generate a hydrophobic MIL, immiscible with the aqueous phase and capable of extracting DNA. The use of these in situ formed MILs in DNA extractions pose many advantages over existing methodologies such as high extraction efficiencies and simple manipulation of the MIL due to low viscosity. Another significant bottleneck in DNA extraction procedures is the recovery of extracted DNA within the MIL. Methods directly coupling DNA extraction to downstream analysis such as PCR have been developed [18, 20]. Although carefully designed PCR buffers were able to alleviate any inhibition caused by the MIL, it is important to evaluate the effect each MIL has on the fluorescence signal in downstream applications due to their paramagnetic nature and so that fluorescence-compatible MILs can be identified.

1.3. Organization of the Thesis

This main goal of this thesis is to apply a new generation of MILs for the extraction of DNA and investigate their fluorescence quenching effects for use in bioanalytical applications. Based on these main objectives, the thesis is divided into the following chapters:

- **Chapter 2** describes the extraction of different sized fragments of double-stranded DNA (dsDNA) using *in situ* MIL-DLLME and conventional MIL-DLLME. The extraction procedure was coupled to high-performance liquid chromatography with diode array detection (HPLC-DAD) and fluorescence emission spectroscopy. Higher extraction efficiencies were found for the *in situ* formed MILs in comparison to conventional MILs, both containing the paramagnetic component in the cation, and a previous generation of MIL, with the paramagnetic component in the anion.

- **Chapter 3** investigates the fluorescence quenching of the *in situ* formed MILs with SYBR Green I bound with dsDNA, as the fluorophore complex. Förster Resonance Energy Transfer and Stern-Volmer models were used to evaluate the fluorescence quenching effects of each component of the MIL structure.
- **Chapter 4** provides a brief summary of the work.

1.4. References

1. Reece JB, Urry LA, Cain ML, Wasserman SA, Minorsky P V., Jackson RB (2011) Campbell Biology, 9th ed. Pearson Education, Inc., San Francisco, CA, USA
2. Mouliere F, El Messaoudi S, Pang D, Dritschilo A, Thierry AR (2014) Multi-marker analysis of circulating cell-free DNA toward personalized medicine for colorectal cancer. Mol Oncol 8:927–941 . doi: 10.1016/j.molonc.2014.02.005
3. Horsman KM, Bienvenue JM, Blasier KR, Landers JP (2007) Forensic DNA analysis on microfluidic devices: A review. J Forensic Sci 52:784–799 . doi: 10.1111/j.1556-4029.2007.00468.x
4. Ansorge WJ (2009) Next-generation DNA sequencing techniques. N Biotechnol 25:195–203 . doi: 10.1016/j.nbt.2008.12.009
5. Caldwell JM (2017) Food Analysis Using Organelle DNA and the Effects of Processing on Assays. Annu Rev Food Sci Technol 8:57–74 . doi: 10.1146/annurev-food-030216-030216
6. Tan SC, Yiap BC (2009) DNA, RNA, and Protein Extraction: The Past and The Present. J Biomed Biotechnol 2009:1–10 . doi: 10.1155/2009/574398
7. Lienhard A, Schäffer S (2019) Extracting the invisible: obtaining high quality DNA is a challenging task in small arthropods. PeerJ 7:1–17 . doi: 10.7717/peerj.6753
8. Ventura SPM, E Silva FA, Quental M V., Mondal D, Freire MG, Coutinho JAP (2017) Ionic-Liquid-Mediated Extraction and Separation Processes for Bioactive Compounds: Past, Present, and Future Trends. Chem Rev 117:6984–7052 . doi: 10.1021/acs.chemrev.6b00550
9. Clark KD, Emaus MN, Varona M, Bowers AN, Anderson JL (2018) Ionic liquids: solvents and sorbents in sample preparation. J Sep Sci 41: . doi: 10.1002/jssc.201700864
10. Liu H, Dasgupta PK (1996) Analytical chemistry in a drop. solvent extraction in a microdrop. Anal Chem 68:1817–1821 . doi: 10.1021/ac960145h

11. Clark KD, Nacham O, Yu H, Li T, Yamsek MM, Ronning DR, Anderson JL (2015) Extraction of DNA by magnetic ionic liquids: Tunable solvents for rapid and selective DNA analysis. Anal Chem 87:1552–1559 . doi: 10.1021/ac504260t

12. An J, Rahn KL, Anderson JL (2017) Headspace single drop microextraction versus dispersive liquid-liquid microextraction using magnetic ionic liquid extraction solvents. Talanta 167:268–278 . doi: 10.1016/j.talanta.2017.01.079

13. Zhang Z, Yang MJ, Pawliszyn J (1994) Solid-Phase Microextraction: A Solvent-Free Alternative for Sample Preparation. Anal Chem 66:844A-853A . doi: 10.1021/ac00089a001

14. Rezaee M, Assadi Y, Milani Hosseini M-R, Aghaee E, Ahmadi F, Berijani S (2006) Determination of organic compounds in water using dispersive liquid–liquid microextraction. J Chromatogr A 1116:1–9 . doi: 10.1016/j.chroma.2006.03.007

15. Clark KD, Nacham O, Purslow JA, Pierson SA, Anderson JL (2016) Magnetic ionic liquids in analytical chemistry: A review. Anal Chim Acta 934:9–21 . doi: 10.1016/j.aca.2016.06.011

16. Yao C, Anderson JL (2009) Dispersive liquid-liquid microextraction using an in situ metathesis reaction to form an ionic liquid extraction phase for the preconcentration of aromatic compounds from water. Anal Bioanal Chem 395:1491–1502 . doi: 10.1007/s00216-009-3078-0

17. Bowers AN, Trujillo-Rodríguez MJ, Farooq MQ, Anderson JL (2019) Extraction of DNA with magnetic ionic liquids using in situ dispersive liquid – liquid microextraction. Anal Bioanal Chem

18. Emaus MN, Clark KD, Hinners P, Anderson JL (2018) Preconcentration of DNA using magnetic ionic liquids that are compatible with real-time PCR for rapid nucleic acid quantification. Anal Bioanal Chem 4135–4144 . doi: 10.1007/s00216-018-1092-9

19. Emaus MN, Varona M, Anderson JL (2019) Sequence-specific preconcentration of a mutation prone KRAS fragment from plasma using ion-tagged oligonucleotides coupled to qPCR compatible magnetic ionic liquid solvents. Anal Chim Acta 1068:1–10 . doi: 10.1016/j.aca.2019.04.005

20. Clark KD, Yamsek MM, Nacham O, Anderson JL (2015) Magnetic ionic liquids as PCR-compatible solvents for DNA extraction from biological samples. Chem Commun 51:16771–16773 . doi: 10.1039/c5cc07253k

CHAPTER 2. EXTRACTION OF DNA WITH MAGNETIC IONIC LIQUIDS USING *IN SITU* DISPERSIVE LIQUID-LIQUID MICROEXTRACTION

Ashley N. Bowers, María J. Trujillo-Rodríguez, Muhammad Q. Farooq, and

Jared L. Anderson

Department of Chemistry, Iowa State University, Ames, Iowa 50011 USA

Modified from a manuscript published in Analytical and Bioanalytical Chemistry

2.1. Abstract

A new class of magnetic ionic liquids (MILs) with metal-containing cations was applied in in situ dispersive liquid-liquid microextraction (DLLME) for the extraction of long and short double-stranded DNA. For developing the method, MILs comprised of N-substituted imidazole ligands (with butyl-, benzyl-, or octyl-groups as substituents) coordinated to different metal centers (Ni^{2+}, Mn^{2+} or Co^{2+}) as cations, and chloride anions were investigated. These water-soluble MILs were reacted with the bis[(trifluoromethyl)sulfonyl]imide anion during the extraction to generate a water immiscible MIL capable of preconcentrating DNA. The feasibility of combining the extraction methodology with anion-exchange high performance liquid chromatography with diode array detection (HPLC-DAD) or fluorescence spectroscopy was studied. The method with the Ni^{2+} and Co^{2+}-based MILs was easily combined with fluorescence spectroscopy and provided a faster and more sensitive method than HPLC-DAD for the determination of DNA. In addition, the method was compared to conventional DLLME using analogous water immiscible MILs. The developed in situ MIL-DLLME method required only 3 min for DNA extraction and yielded 1.1-1.5 times higher extraction efficiency (EFs) than the conventional MIL-DLLME method. The *in situ* MIL-DLLME method was also compared to the trihexyl(tetradecyl)phosphonium tris(hexafluorocetylaceto)nickelate(II) MIL, which has been used in previous DNA extraction studies. EFs of 42-99% were obtained using the new generation

of MILs, whereas EFs of only 20-38% were achieved with the phosphonium MIL. This new class of MILs are simple and inexpensive to prepare. In addition, the MILs present operational advantages such as easier manipulation in comparison to hydrophobic MILs, which can have high viscosities. These MILs are a promising new class of DNA extraction solvents that can be manipulated using an external magnetic field.

Keywords: DNA; magnetic ionic liquids; in situ dispersive liquid-liquid microextraction; high performance liquid chromatography; fluorescence spectroscopy

2.2. Introduction

DNA is often regarded as the central database of the cell, controlling cell growth, maintenance, and replication [1]. DNA analysis is routinely used in many fields including forensics [2], anthropology [3], clinical diagnostics [4], genetics [5] and pharmaceuticals [6]. Isolating genomic DNA from cells is often the first step in numerous molecular biology procedures used in these fields such as quantitative polymerase chain reaction (qPCR), gene expression, and gene therapy [7, 8]. These techniques require high quality DNA and their success is often affected by DNA purity and integrity [9]. Obtaining high yields and pure DNA from complex biological matrices presents a significant sample preparation challenge in nucleic acid analysis.

Current methodologies for nucleic acid purification involve solution-based or column-based protocols [7]. Many commercially available kits use solid or semisolid sorbent phases such as anion-exchange spin columns, silica-based membranes, and magnetic particles [7]. However, these kits often are very expensive and have limited reusability. Conventional liquid-liquid extraction (LLE) approaches to purify nucleic acids use phenol and chloroform [7]. Although high quality nucleic acid can be obtained, some organic solvents such as phenol and chloroform can be toxic and environmentally unfriendly. In order to reduce the use of harmful organic

solvents and provide selectivity in the extraction, ionic liquids (ILs), and their magnetic analogs, magnetic ionic liquids (MILs), have grown in popularity as extraction solvents over the past decade [10–18].

ILs are molten salts with melting points below 100 ºC and are comprised entirely of ions [19]. ILs have negligible vapor pressure at room temperature, relatively high thermal stability, as well as variable viscosity [13]. MILs are a subclass of ILs which contain a paramagnetic metal in the cation or anion, allowing the compound to possess magnetic properties [10]. The cationic and anionic moieties of ILs and MILs can often be tuned for specific applications, including for nucleic acid extractions [11, 20, 21].

Previous studies have used ILs or IL-modified materials [22] in different extraction and microextraction techniques for nucleic acids, including single drop microextraction (SDME) [21, 23], dispersive liquid-liquid microextraction (DLLME) [20, 21, 23–27], aqueous biphasic systems (ABS) [28, 29] and solid-phase microextraction (SPME) [30–34]. SPME often requires long extraction and desorption times; therefore, IL-based liquid-phase extraction techniques such as DLLME are generally preferred [35]. Conventional DLLME involves the rapid injection of a mixture of extraction and dispersive solvents into an aqueous sample, resulting in the enrichment of analytes from the sample matrix [36]. In this technique, a hydrophobic IL is typically used as the extraction solvent. However, the use of MILs containing paramagnetic anions has also been described [37, 38]. In this case, magnetic separation of the MIL can be performed after DLLME, which simplifies the overall procedure. In a variation of the technique called *in situ* DLLME, a hydrophilic IL is mixed with a metathesis reagent, promoting an anion-exchange reaction that generates a hydrophobic IL. This reaction creates numerous finely dispersed hydrophobic IL microdroplets capable of interaction with analytes. The anion-exchange process also increases

the surface area of the IL extraction solvent, generally leading to higher extraction efficiencies [17, 39, 40]. The use of MILs for *in situ* DLLME was recently possible due to the design of MILs that possess a paramagnetic component in the cation of their structure [41–43]. Since the paramagnetic component is within the cation of the MIL, it is not exchanged during the metathesis reaction allowing magnetic separation to be performed.

This study constitutes the first report of *in situ* DLLME using MILs for the extraction of DNA. The optimal extraction efficiency of different DNA sizes was investigated using ten types of MILs. The extraction procedure is combined with high performance liquid chromatography with diode array detection (HPLC-DAD) and fluorescence emission spectroscopy. The superior extraction performance of the developed *in situ* MIL-DLLME method is confirmed by its comparison with conventional DLLME using both MILs with the paramagnetic component in the cation and a previous generation of MIL, with the paramagnetic component in the anion. MILs developed *in situ* demonstrated superior extraction efficiency and are easier to work with in comparison to hydrophobic MILs, which can have high viscosities and are difficult to pipette [10, 44–46].

2.3. Experimental

2.3.1. Chemicals, Reagents, Materials

Different sized fragments of double-stranded DNA (dsDNA) (~20 kbp salmon testes DNA, stDNA; ~250-500 bp stDNA; and 20 bp DNA) were employed in this study. stDNA (approximately 20 kbp) was acquired from Sigma-Aldrich (St. Louis, MO, USA). To generate shorter duplex DNA fragments of approximately 250 to 500 bp, stDNA was sheared for 60 cycles (1 cycle: 30 s on and 30 s off) through sonication in an ice bath. Agarose from LabExpress (Ann Arbor, MI, USA) at 1% w/v concentration was employed for electrophoretic separation to confirm the size of the sheared stDNA fragments. SYBR Safe DNA gel stain was

purchased from Invitrogen (Waltham, MA, USA). A l Kb Plus DNA Ladder was purchased from Gold Biotechnology (St. Louis, MO, USA). A synthetic oligonucleotide (sequence: 5'-AGG GCG TGA ATG TAA GCG TG-3' annealed to its complementary strand) was purchased from Integrated DNA Technologies (Coralville, IA, USA). Ethylenediaminetetraacetic acid (EDTA, ACS reagent, 99.4-100.06%) was purchased from Sigma-Aldrich. Tris(hydroxymethyl)aminomethane (Tris base) and the corresponding hydrochloride salt (Tris-HCl) were purchased from Research Products International (Mount Prospect, IL, USA). SYBR Green I (10000X) was purchased from Life Technologies (Eugene, OR, USA). Sodium chloride (100.1%), sodium hydroxide (99.4%) and N,N-dimethylformamide (99.9%) were purchased from Fisher Scientific (Fair Lawn, NJ, USA). Ultrapure water (18.2 MΩ·cm) was obtained from a Milli-Q water purification system (Millipore, Bedford, MA, USA).

For the synthesis of MILs, the reagents cobalt(II) chloride (97%), acetonitrile (99.9%) and 1-butylimidazole (98%) were purchased from Sigma-Aldrich. Nickel(II) chloride (98%), 1-benzylimidazole (99%), 1,1,1,5,5,5-hexafluoroacetylacetone (99%), and ammonium hydroxide (28-30% solution in water) were purchased from Acros Organics (Morris Plains, NJ, USA). Manganese(II) chloride tetrahydrate (98.0-101.0%) was purchased from Alfa Aesar (Ward Hill, MA, USA). Trihexyl(tetradecyl)phosphonium chloride (97.7%) was purchased from Strem Chemicals (Newburyport, MA, USA). Lithium bis[(trifluoromethyl)sulfonyl]imide ($[Li^+][NTf_2^-]$) was purchased from SynQuest Laboratories (Alachua, FL, USA). Anhydrous diethyl ether (99.0%) was purchased from Avantor Performance Materials Inc. (Center Valley, PA, USA). Ethyl alcohol was purchased from Decon Laboratories, Inc. (King of Prussia, PA, USA).

Chemical structures of the ten different MILs examined in this study are shown in Figure 1. Nine of the MILs have a general chemical structure based on a cation comprised of four N-

substituted imidazole ligands (RIm, with R = B for butyl-, Bn for benzyl-, and O for octyl-) coordinated to different metal centers (M = Ni^{2+}, Mn^{2+} or Co^{2+}), and chloride or bis[(trifluoromethyl)sulfonyl]imide ($[NTf_2^-]$) anions. The water-soluble MILs ($[Ni(BIm)_4^{2+}]2[Cl^-]$, $[Ni(BnIm)_4^{2+}]2[Cl^-]$, $[Mn(BIm)_4^{2+}]2[Cl^-]$ and $[Co(BIm)_4^{2+}]2[Cl^-]$) were used for *in situ* DLLME. The corresponding hydrophobic form of these MILs were generated by a metathesis reaction with $[Li^+][NTf_2^-]$ and used in conventional DLLME. Stock solutions of the MILs in chloride anion form were prepared in ultrapure water at a concentration of 20 $mg \cdot mL^{-1}$, except for the $[Ni(BIm)_4^{2+}]2[Cl^-]$ MIL, which had a concentration of 25 $mg \cdot mL^{-1}$. An aqueous solution of $[Li^+][NTf_2^-]$ containing a concentration of 600 $mg \cdot mL^{-1}$ was used for *in situ* DLLME. To compare to previous MILs used in DNA extractions, the trihexyl(tetradecyl)phosphonium tris(hexafluorocetylaceto)nickelate(II) ($[P_{66614}^+][Ni(II)(hfacac)_3^-]$) MIL was used, which is hydrophobic and is composed of Ni(II) coordinated to three hexafluoroacetylacetonate ($[hfacac^-]$) ligands in the anion.

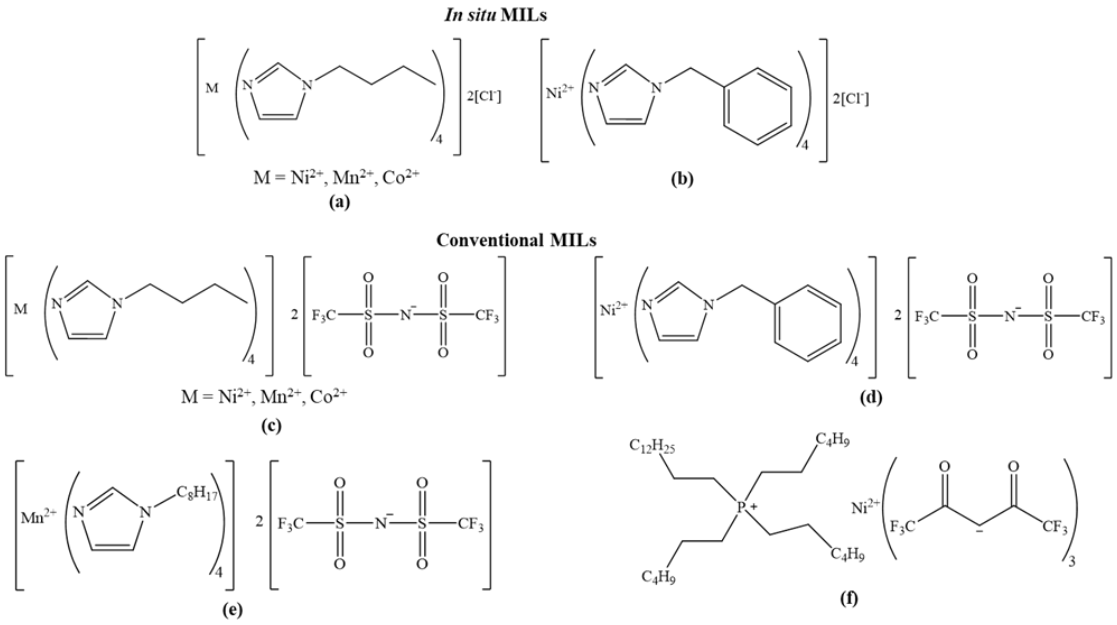

Figure 1. Chemical structures of the MILs examined in this study (a) $[Ni(BIm)_4^{2+}]2[Cl^-]$, $[Mn(BIm)_4^{2+}]2[Cl^-]$ and $[Co(BIm)_4^{2+}]2[Cl^-]$). (b) $[Ni(BnIm)_4^{2+}]2[Cl^-]$. (c) $[Ni(BIm)_4^{2+}]2[NTf_2^-]$,

$[Mn(BIm)_4^{2+}]2[NTf_2^-]$ and $[Co(BIm)_4^{2+}]2[NTf_2^-]$. (d) $[Ni(BnIm)_4^{2+}]2[NTf_2^-]$. (e) $[Mn(OIm)_4^{2+}]2[NTf_2^-]$. (f) $[P_{66614}^+][Ni(II)(hfacac)_3^-]$.

2.3.2. Instrumentation

An Agilent Technologies 1260 Infinity high-performance liquid chromatograph (Santa Clara, USA) consisting of a quaternary pump, a column thermostat, manual injector and diode array detector (DAD) was used for the indirect determination of DNA. All chromatographic separations were performed using an anion exchange column (TSKgel DEAE-NPR, 35 mm × 4.6 mm i.d., 2.5 µm) equipped with a guard column (TSKgel DEAE-NPR, 5 mm × 4.6 mm i.d., 5 µm) from Tosoh Bioscience (King of Prussia, PA, USA). Mobile phase comprised of (A) 20 mM Tris-HCl (pH 8) and (B) 1 M NaCl/20 mM Tris-HCl (pH 8) at a flow rate of 0.5 $mL \cdot min^{-1}$ was employed for the separations. Gradient elution was performed by increasing from 20% to 100% B over 20 min, and detection at 260 nm. The column was maintained at 40 ºC.

Fluorescence emission spectra were acquired using a Synergy H1 Multi-Mode microplate reader (Winooski, VT, USA) and 384-well plate, black polystyrene, flat bottom microplates (Corning, Corning, NY, USA). Fluorescence emission measurements were obtained at an excitation wavelength of 480 nm. The emission intensity was scanned from 510 nm to 650 nm with 1 nm resolution. Measurements were acquired in top-read mode.

A Shimadzu AA-7000 atomic absorption spectrophotometer (AAS) equipped with an ASC-7000 auto sampler (Kyoto, Japan) was used for AA measurements. Nickel and manganese Atomax hollow cathode lamps (PerkinElmer, MedTech Park, Singapore) were used for the determination of nickel and manganese content, respectively. Likewise, a cobalt hollow cathode lamp (Hamamatsu Photonics K.K., Beijing, China) was used for the detection of cobalt.

2.3.3. Procedures

2.3.3.1. Synthesis of magnetic ionic liquids

The $[P_{66614}^{+}][Ni(II)(hfacac)_3^{-}]$ MIL was synthesized and purified following a previously reported procedure [47]. The MILs used for *in situ* and conventional DLLME were synthesized according to a recently reported procedure [41]. The $[Ni(BnIm)_4^{2+}]2[Cl^{-}]$ MIL was synthesized following the same procedure, except 3.16 mmol of $NiCl_2$ was added to 12.64 mmol of 1-benzylimidazole in a round bottom flask with 10 mL of water and refluxed at 80 ºC for 12 hours. The solvent was removed under reduced pressure at 40 ºC, and the MIL product was washed with diethyl ether and dried in a vacuum oven for 24 hours at 40 ºC.

2.3.3.2. In situ dispersive liquid-liquid microextraction

A general schematic of the *in situ* DLLME process is shown in Figure 2. All extractions were performed in 4 mL clear glass vials with a screw hole cap containing a polytetrafluoroethylene (PTFE)/silicone septum (Supelco, Bellefonte, PA). An aqueous solution of the MIL in the chloride form (17 to 24 µmol) was added to an aqueous solution of DNA (~20 kbp stDNA, ~250-500 bp stDNA or 20 bp DNA). The DNA concentration and the total extraction volume were kept constant at 2 nM and 2 mL, respectively. A volume of 300 µL of dimethylformamide was then added as a dispersive solvent. The vial was homogeneously mixed with a vortex from Fisher Scientific at 2100 rpm for 10 seconds, followed by the addition of the $[Li^{+}][NTf_2^{-}]$ anion-exchange reagent at a MIL: $[Li^{+}][NTf_2^{-}]$ molar ratio of 1:1.5, 1:2, 1:2.5 or 1:2.8, depending on the experiment. The vial was then mixed by vortex for 3 min to facilitate the metathesis reaction and form a hydrophobic MIL droplet. After droplet formation, the *in situ* generated hydrophobic MIL settled at the bottom of the vial, and an aliquot of the upper aqueous phase was used for indirect determination of the DNA extraction efficiency (EF) by HPLC-DAD

or fluorescence emission spectroscopy. The specific conditions for each MIL are shown in Table A1 of Appendix A.

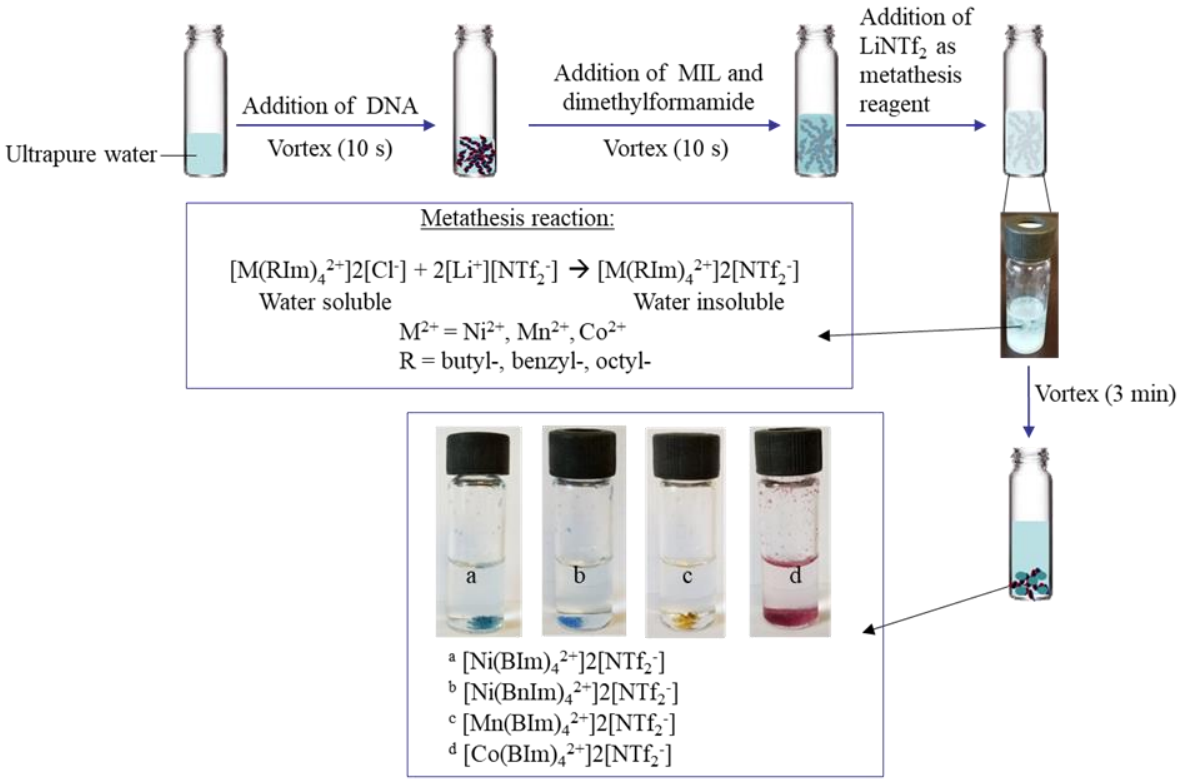

Figure 2. Schematic describing the *in situ* DLLME method using MILs for the extraction of DNA.

2.2.3.3. Conventional dispersive liquid-liquid microextraction

The overall process for the conventional DLLME method is shown in Figure A1 of Appendix A. An amount of 16 to 21 µmol of the hydrophobic MIL (in [NTf2-] form) was dissolved in 300 µL of dimethylformamide as a dispersive solvent. The mixture was then added to a 2 nM aqueous solution of DNA (~20 kbp stDNA, ~250-500 bp stDNA or 20 bp DNA) in a 4 mL extraction vial and homogeneously vortexed at 2100 rpm for 5 min to promote dispersion of the hydrophobic MIL throughout the aqueous phase containing the DNA. The MIL was allowed

to settle at the bottom of the vial and an aliquot of the aqueous phase was taken for indirect determination of DNA EF by HPLC-DAD or fluorescence emission spectroscopy. The same procedure was followed for the $[P_{66614}^{+}][Ni(II)(hfacac)_3^{-}]$ MIL, except 15 µmol of the MIL was directly added to the aqueous DNA solution without the addition of dimethylformamide, to prevent the MIL from dissolving completely without droplet formation. The amount of each MIL used for extractions are provided in Table A2 of Appendix A.

2.2.3.4. Determination of extracted DNA and free metal remaining in aqueous phase

Indirect determination of the extracted DNA was performed by two different methods: HPLC-DAD and fluorescence spectroscopy. HPLC-DAD separation and detection of the DNA was performed by injecting 20 µL of the aqueous phase after extraction to the system using the conditions detailed in Section 2.3.2. Fluorescence emission spectra were obtained by adding 0.2 µL of a 50× SYBR Green I stock solution to a 9.8 µL aliquot of the aqueous phase after extraction. The SYBR Green I dye and the aqueous phase aliquot was mixed for 5 s with a vortex mixer (Barnstead Thermolyne Type 16700, Dubuque, IA, USA) and centrifuged for 3 s (Eppendorf Centrifuge 5424, Hamburg, Germany). The solutions were transferred to the wells in a black microplate and measurements were performed in triplicate at room temperature (~23 ºC).

Flame atomic absorption spectroscopy (FAAS) was performed to determine the amount of metal remaining in the aqueous phase after the in situ DLLME procedure. The method of standard addition was employed by adding a fixed volume of 250 µL of the aqueous phase after in situ DLLME to different $NiCl_2$, $MnCl_2$ or $CoCl_2$ standards with concentrations ranging between 0-100 µM.

2.4. Results and Discussion

2.4.1. Comparison of stDNA Extraction Efficiency Using Different Methods

In this study, up to 10 different MILs were applied in two different extraction methods (in situ DLLME and conventional DLLME). Different MIL: $[Li^+][NTf_2^-]$ molar ratios were selected for performing *in situ* DLLME experiments, as explained in Section 2.3.3.2. Different molar ratios were needed, based on the nature of the MIL and in order to obtain a magnetic liquid after the metathesis reaction. HPLC-DAD was initially studied as the separation and indirect detection method. However, this approach was time consuming, required greater amounts of solvents, and frequent cleaning of the column to prevent analyte carryover. Pressure issues in the system were observed after subsequent injections. This problem was likely due to interactions with components remaining in the aqueous phase after extraction (such as the MIL, metal, ligands and unreacted $[Li^+][NTf_2^-]$). Another possible reason for pressure issues could be the weak anion exchange groups modified on the surface of the stationary phase. Fluorescence emission spectroscopy was studied as an alternative to HPLC-DAD and was found to be simpler and required less solvent. In both methods, the aforementioned components remaining in the aqueous phase after extraction can possibly affect the signal.

A comparison of the results obtained with these two analytical techniques was carried out for all extractions performed with different MILs. These experiments were performed with stDNA spiked samples. The EF was calculated using Eq. (1).

$$EF = \left(1 - \frac{P_{aq}}{P_{std}}\right) \times 100 \qquad \text{Eq. (1)}$$

where P_{aq} is the peak area of DNA in the aqueous phase after extraction in HPLC-DAD or the

mean maximum relative fluorescence units (mean max. RFU) obtained from the emission spectrum in fluorescence measurements. Similarly, P_{std} is the peak area or mean max. RFU obtained from measurement of a 2 nM DNA standard solution, which corresponds to the initial DNA concentration used in extractions. A comparison of the EF values was established by using the Student's t-test at a 95% confidence level (Table A3 of Appendix A). In general, no significant EF differences were found for various MILs using the HPLC-DAD or fluorescence emission detection methods (Table A3 and Figure A3 of Appendix A). These results indicate that SYBR Green I underwent a selective interaction with the DNA remaining after extraction, and no other component of the aqueous sample caused an interference in the determination. An exception of this behavior was observed with the $[Mn(BIm)_4^{2+}]2[Cl^-]$ MIL for which the performed statistical analysis revealed differences between the detection methods, likely due to the formation of Mn(II,III) oxide precipitates (i.e., MnO, Mn_2O_3, MnO_2, and Mn_2O_7 [48]). In fact, the formation of a precipitate was observed after storing aqueous solutions of $[Mn(BIm)_4^{2+}]2[Cl^-]$ longer than 2 h. The $[Mn(BIm)_4^{2+}]2[Cl^-]$ MIL precipitate was characterized by Raman spectroscopy and X-ray diffraction (XRD) and compared to those of manganese(II) oxide and manganese(III) oxide. Both the Raman spectrum and XRD pattern of the $[Mn(BIm)_4^{2+}]2[Cl^-]$ MIL precipitate and Mn(II,III) oxides were similar (Figure A6 of Appendix A). $[Mn(BIm)_4^{2+}]2[Cl^-]$ was the only MIL in which the formation of precipitate was observed, likely due to the weaker stability of Mn(II) imidazole complexes compared to the analogous Co(II)- and Ni(II)-imidazole complexes. The reported stability constants (log *K*), found through potentiometric pH titrations (I = 0.5 M, $NaNO_3$; 25 °C), were 1.42 ± 0.01, 2.48 ± 0.02 and 3.09 ± 0.01, for the complexes $[MnIm^{2+}]$, $[CoIm^{2+}]$ and $[NiIm^{2+}]$, respectively [49]. With these considerations, HPLC-DAD was chosen to perform indirect detection of DNA with all of the

studied Mn(II)-based MILs, including $[Mn(BIm)_4^{2+}]2[Cl^-]$, $[Mn(BIm)_4^{2+}]2[NTf_2^-]$ and $[Mn(OIm)_4^{2+}]2[NTf_2^-]$.

The Student's t-test was not used to compare detection methods for the $[Ni(BnIm)_4^{2+}]2[Cl^-]$, $[Co(BIm)_4^{2+}]2[Cl^-]$ and $[Co(BIm)_4^{2+}]2[NTf_2^-]$ MILs because no stDNA was detected in HPLC-DAD. These results indicated almost quantitative extraction of the DNA, but also that the indirect method was not the most suitable for studying the extraction performance of the DLLME methods. The data obtained with the benzylimidazole-based MILs using HPLC-DAD agreed with those obtained by fluorescence, for which an EF up to 99% was obtained, indicating quantitative extraction of stDNA.

Figure 3 shows the EF obtained for the extraction of 3 different DNA sizes with all MILs. The extraction method was combined with HPLC-DAD or fluorescence and the detection method was based on the aforementioned considerations (i.e., experiments using $[Mn(BIm)_4^{2+}]2[Cl^-]$, $[Mn(BIm)_4^{2+}]2[NTf_2^-]$ and $[Mn(OIm)_4^{2+}]2[NTf_2^-]$ MILs were analyzed by HPLC-DAD, and the remaining MILs using fluorescence spectroscopy). Relative standard deviations (RSD) lower than 20% were obtained in all cases except for the Mn(II)-based MILs, where RSD values below 25% were achieved. The obtained EF values were 1.1-1.5 times higher when *in situ* DLLME was employed compared to conventional DLLME, an increase that is directly related to the metathesis reaction. These results were in agreement with previously reported *in situ* DLLME methods [39, 40, 42, 43, 50]. Furthermore, in both methods the use of dimethylformamide as disperser solvent and vortex mixing increased the dispersion of the hydrophobic MIL in the aqueous solution, maximizing the contact area between the aqueous solution and MIL (see Figure 3).

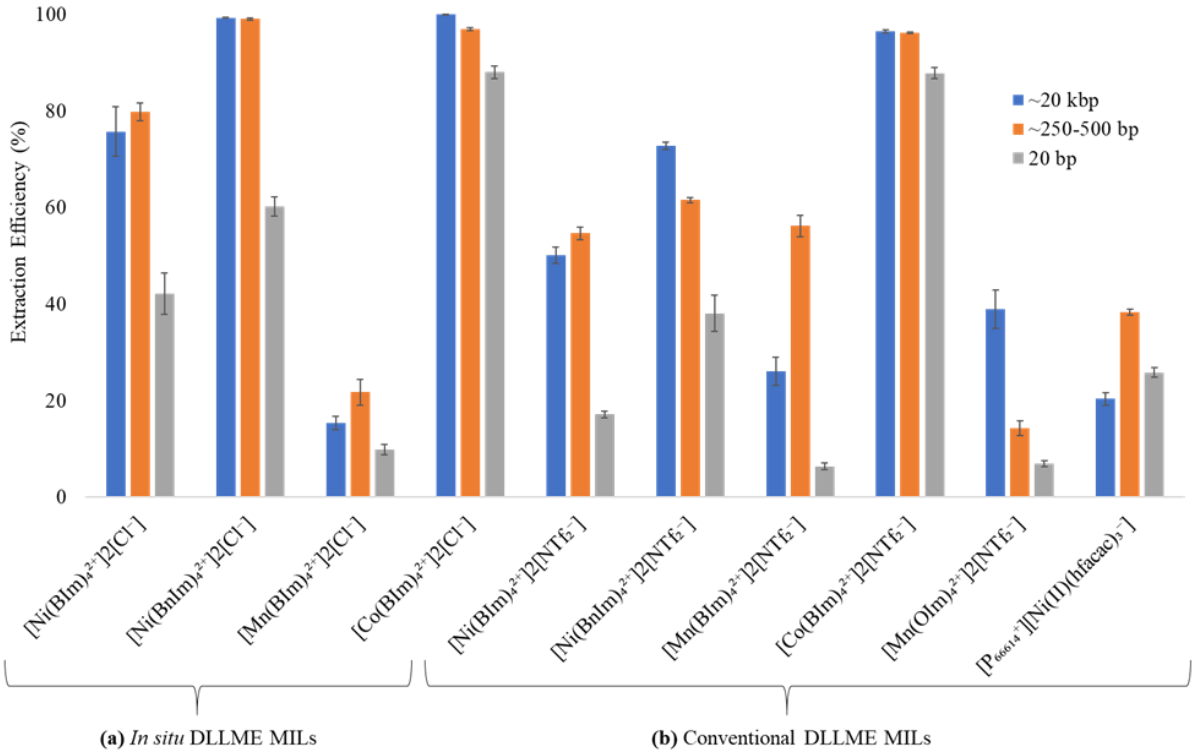

Figure 3. Extraction efficiencies (% EF) of ~20 kbp stDNA (blue), ~250-500 bp stDNA (orange) and 20 bp DNA (gray) fragments by each of the MILs using **(a)** MIL-based *in situ* DLLME or **(b)** conventional MIL-DLLME and fluorescence emission spectroscopy detection. Experimental conditions (n = 3): 2 nM DNA, 2 mL total extraction volume, 15-24 µmol MIL, 300 µL dimethylformamide dispersive solvent, 3 min vortex at 2100 rpm. Note: For *in situ* DLLME, a range of 1:1.5 to 1:2.8 molar ratio of MIL:$[Li^+][NTf_2^-]$ was used, depending on the MIL. For the $[P_{66614}^+][Ni(II)(hfacac)_3^-]$ MIL, no dispersive solvent was used. HPLC-DAD detection was used for the $[Mn(BIm)_4^{2+}]2[Cl^-]$ MIL.

2.4.2. Effect of the MIL Structure on the Extraction of DNA

The DLLME methods described in this work are influenced by the metal center and the ligands that comprise the MIL. The transition metal center within the cation of the MIL can interact with DNA primarily through electrostatic interactions of the negatively charged phosphate backbone of DNA and through metal binding to the nitrogenous bases of DNA [51, 52]. Additionally, MILs and DNA can interact through hydrogen bonding, π-π stacking and van

der Waals interactions [53]. IL/MIL cations can bind to the minor grooves of dsDNA through hydrophobic and polar interactions [54]. According to Figure 3, the Co(II)-based MILs provided the highest EF values (87% or greater), with almost quantitative extraction of ~20 kbp and ~250-500 bp DNAs using both *in situ* and conventional DLLME. The extractions using Mn(II)-based MILs provided lower EF values, likely due to the weaker stability of the MIL (see Section 2.4.1).

The substituent groups attached to the imidazole rings within the MIL structure also play a role in the extraction of DNA. Most of the MILs contained BIm as ligand, with the exception of two MILs that contained BnIm (i.e., $[Ni(BnIm)_4^{2+}]2[Cl^-]$, and $[Ni(BnIm)_4^{2+}]2[NTf_2^-]$), and one composed of OIm (i.e., $[Mn(OIm)_4^{2+}]2[NTf_2^-]$). The $[Mn(OIm)_4^{2+}]2[NTf_2^-]$ MIL was only applied for conventional DLLME because its corresponding chloride salt ($[Mn(OIm)_4^{2+}]2[Cl^-]$) was not water soluble; therefore, the metathesis reaction with the DNA spiked sample was not successful. In both extraction modes, higher EF values were obtained with Ni(II)-based MILs containing BnIm as opposed to BIm ligands. In these cases, the BnIm ligands not only provided a more hydrophobic MIL structure but also facilitated π- π stacking of the MIL with DNA. In conventional MIL-DLLME, the $[Mn(OIm)_4^{2+}]2[NTf_2^-]$ MIL provided higher EF than $[Mn(BIm)_4^{2+}]2[NTf_2^-]$ for the extraction of ~20 kbp stDNA, providing evidence that imparting more hydrophobicity to the MIL through the addition of longer alkyl chains substituents to the imidazole ligand can enhance the extraction of larger DNA fragments.

Results obtained using this new generation of MILs were also compared to the $[P_{66614}^+][Ni(II)(hfacac)_3^-]$ MIL, which has been used in previous studies for DNA extractions [23, 25, 55]. In general, higher EF values were obtained for most of the new generation MILs, including those used in both *in situ* MIL-DLLME and conventional MIL-DLLME. For these materials, the paramagnetic metal is within the cation rather than the anion, and therefore *in situ*

generation of the hydrophobic MIL was possible without exchanging the paramagnetic metal during the metathesis reaction. Higher EF values were also obtained for the MILs containing [NTf_2^-] anions used in conventional MIL-DLLME compared to the [P_{66614}^+][$Ni(II)(hfacac)_3^-$] MIL. This may be due to greater electrostatic interaction between the divalent metal in the cation and the negatively charged phosphate groups in the DNA backbone, rather than with the trihexyl(tetradecyl)phosphonium cation of the [P_{66614}^+][$Ni(II)(hfacac)_3^-$] MIL.

2.4.3. Selectivity of MILs in the Extraction of Duplex DNA Fragments of Varying Size

The selectivity of the MILs in the extraction of different sized fragments of double-stranded DNA was investigated, and the results are shown in Figure 3. In general, similar EF values for each MIL were observed in the extraction of the ~20 kbp stDNA and the ~250-500 bp DNA fragments. However, the EF values were partially reduced when the method was applied for the extraction of 20 bp DNA. The larger-sized DNA fragments (~20 kbp stDNA and ~250-500 bp DNA) provided a more hydrophobic environment, which increased hydrophobic interactions between the DNA and the MIL. Consequently, more DNA was extracted compared to the 20 bp DNA fragments, which are smaller and less hydrophobic. The biggest differences in EF were found with the Ni(II)-based MILs. Higher EF values (between 75-99%) were observed for the extraction of ~20 kbp stDNA and ~250-500 bp DNA fragments with the [$Ni(BIm)_4^{2+}$]2[Cl^-] and [$Ni(BnIm)_4^{2+}$]2[Cl^-] MILs, whereas EF values ranging between 42-60% were obtained for the 20 bp DNA fragment. The same trend was observed for the [$Ni(BIm)_4^{2+}$]2[NTf_2^-] and [$Ni(BnIm)_4^{2+}$]2[NTf_2^-] MILs with EF values between 50-73% for the larger DNA fragments and between 20-32% for the 20 bp DNA fragment. The [$Mn(BIm)_4^{2+}$]2[NTf_2^-] MIL extracted the ~250-500 bp DNA fragments with the highest EF value of 56%, whereas the EF dropped to 26% and 8% for the ~20 kbp stDNA and 20 bp DNA fragments, respectively. If the results of this MIL are compared to those obtained for the

$[Mn(OIm)_4^{2+}]2[NTf_2^-]$ MIL, increasing the alkyl chain substituent from butyl to octyl increased the tendency of the MIL to extract DNA fragments of ~20 kbp. For the Co(II)-based MILs, more subtle differences were observed in the extraction of different sizes of DNA.

2.4.4. Determination of Metal Ion Concentration in the Aqueous Phase After Extraction

As previously stated, the key aspect of the *in situ* MIL-DLLME method is the metathesis reaction between the MIL and the metathesis reagent ($[Li^+][NTf_2^-]$). If this reaction is not complete during the extraction procedure, some of the MIL (in the chloride form) can remain unreacted in the aqueous phase. The yield of the metathesis reaction can depend on the extraction conditions, the solubility of the MIL and metathesis reagent in aqueous solution, and the water stability of the MILs. Furthermore, the $[NTf_2^-]$-form of the MIL can also be found in the aqueous phase after extraction, as a result of partial solubility of the MIL in the aqueous solution [56]. In order to verify this hypothesis, AAS using the method of standard addition was applied to determine the amount of metal ion remaining in the aqueous phase after *in situ* MIL-DLLME. Since the metal is within the cation of the MIL, the amount of metal ion remaining in the aqueous phase after extraction can be directly related to the amount of the remaining MIL in both the $[Cl^-]$ and the $[NTf_2^-]$-forms. The obtained results are shown in Figure A7 and Table A4 of Appendix A. The percentage of the MIL in the aqueous phase after extraction, S_{MIL}, was calculated using Eq. (2).

$$S_{MIL} = \frac{C_{aq}}{C_o} \times 100 \qquad \text{Eq. (2)}$$

where C_{aq} is the concentration of the MIL in the aqueous phase after extraction and Co is the initial concentration of MIL. The results indicated that 24–59%, depending on the nature of the

MIL, remained in the aqueous phase after in situ DLLME (Table A4 of Appendix A). Among the different studied MILs, a significant amount of the $[Ni(BIm)_4^{2+}]2[Cl^-]$ MIL was detected in the aqueous phase after extraction (58.8% with respect to the initial amount of spiked MIL). This result is in accordance with the data obtained in Figure 3 which revealed a relatively low EF for this MIL (75.7% for ~20 kbp stDNA), in comparison to the $[Ni(BnIm)_4^{2+}]2[Cl^-]$ and $[Co(BIm)_4^{2+}]2[Cl^-]$ MILs for which almost quantitative extraction of ~20 kbp stDNA was observed. For the $[Ni(BnIm)_4^{2+}]2[Cl^-]$ and $[Co(BIm)_4^{2+}]2[Cl^-]$ MILs, 46.7% and 38.8% of MIL remained in the aqueous phase after extraction, respectively. Nonetheless, for *in situ* DLLME with the three aforementioned MILs, the free MIL in the aqueous phase did not significantly affect the fluorescence signal of DNA as the obtained fluorescence data did not statistically differ with respect to the HPLC-DAD data (Table A3 and Figure A3 of Appendix A). Only 24.2% of the $[Mn(BIm)_4^{2+}]2[Cl^-]$ MIL remained in the aqueous phase, indicating that the Mn(II,III) oxide precipitate that formed over time during the preparation of the solutions for fluorescence detection were likely not present in the aqueous phase during the AAS measurement.

2.4.5. Comparison to Other Reported Methods

DNA extraction by the *in situ* MIL-DLLME method was compared to other IL- and MIL-based extraction methods reported in the literature, and is shown in Table 1. All reported extraction methods provided a high EF of DNA with values around 80% or greater. However, the developed extraction method is rapid, especially if the method is compared with those that used ILs [20, 24], which required centrifugation steps to recover the extraction phase. Among the different methods presented in Table 1 using MILs [21, 23], the present method is faster,

Table 1. Comparison of the developed method with other reported methods from the literature.

Sample/DNA size	Extraction method/ Extraction solvent/sorbent	Analytical technique	Extraction time (min)	EF	Ref.
Aqueous sample/ 20 bp DNA	*In situ* MIL-DLLME/ $[Co(BIm)_4^{2+}]2[Cl^-]$ and $[Li^+][NTf_2^-]$	FD	3	88.05 ± 2.64%	This method
Aqueous sample/ ~250-500 bp stDNA	*In situ* DLLME/ $[Ni(BnIm)_4^{2+}]2[Cl^-]$ and $[Li^+][NTf_2^-]$	FD	3	99.04 ± 0.38%	This method
Aqueous sample/ ~20 kbp stDNA	*In situ* DLLME/ $[Co(BIm)_4^{2+}]2[Cl^-]$ and $[Li^+][NTf_2^-]$	FD	3	99.97 ± 0.03%	This method
Aqueous sample/ ~20 kbp dsDNA	MIL-DDE[a]/ $[P_{6,6,6,14}^+][FeCl_4^-]$	HPLC-UV	30 s	93.8 ± 0.6%	[21]
Aqueous sample/ single-stranded *KRAS* template DNA	MIL-SDME[b]/ $[P_{6,6,6,14}^+][Ni(hfacac)_3^-]$	qPCR	20	-	[23]
Meat samples/ mitochondrial DNA (mtDNA)	IL-ABS[c]/ $[Chol^+][Hex^-]$ (10 w/v%) in sodium phosphate buffer (50 mM, pH = 8.5)	qPCR	15	-	[29]
Maize powder/ genomic DNA (~10 kbp)	IL-ABS[c]/ $[C_2MIm^+][Me_2PO_4^-]$ (10 w/v%) in sodium phosphate buffer (50 mM, pH = 8.5)	qPCR	5 min	--	[28]
Aqueous sample/ ~20 kbp stDNA	*In situ* IL-DLLME/ $[C_{16}POHIm^+][Br^-]$ and $[Li^+][NTf_2^-]$	HPLC-UV	30 min	95.2 ± 0.4%	[20]
Aqueous sample/ calf thymus DNA and salmon testes DNA	IL-DLLME/ $[BMIm^+][PF_6^-]$	FD	10 min	99.5%	[24]

[a] MIL-Based Dispersive Droplet Extraction.
[b] MIL-Based Single-drop Microextraction.
[c] Liquid extraction with an IL-aqueous buffer system.

requiring only 3 min for extraction, with the exception of the method reported by Clark *et al.* that reported an extraction time of 30 s using MIL-based dispersive droplet extraction (MIL-DDE) with the $[P_{6,6,6,14}^{+}][FeCl_4^{-}]$ MIL [21]. In any case, the *in situ* MIL-DLLME method presented in this work is simple to execute due to the low viscosity of the MIL solution in the chloride form, which is used initially in the extraction. Furthermore, this new generation of MILs are easy to prepare and are water stable (except for Mn(II)-based MILs).

2.5. Conclusions

This study constitutes the first report of the *in situ* formation of hydrophobic MILs for the extraction of DNA. This generation of MILs are easy and inexpensive to prepare making them a more affordable alternative for DNA extraction than commercially available DNA extraction kits. At the same time, these MILs possess three important features: (1) paramagnetic nature, resulting in a hydrophobic MIL droplet that can be retrieved with an external magnetic field, (2) their paramagnetic component is in the cation, which allows for the *in situ* generation of the hydrophobic MIL during extraction, and (3) low viscosity, which is convenient for its manipulation and transfer.

The *in situ* MIL-DLLME method can be combined with both HPLC-DAD or fluorescence detection, with the latter method more suitable for faster detection of DNA. Different sized fragments of dsDNA (20 bp, ~250-500 bp and ~20 kbp DNA) were extracted by *in situ* MIL-DLLME and conventional MIL-DLLME where 1.1-1.5 times higher EFs were obtained using *in situ* MIL-DLLME. Among the different studied MILs, the Co-based MILs ($[Co(BIm)_4^{2+}]2[Cl^{-}]$ and $[Co(BIm)_4^{2+}]2[NTf_2^{-}]$) provided the highest EFs (>85%). The Ni-based MILs ($[Ni(BIm)_4^{2+}]2[Cl^{-}]$, $[Ni(BIm)_4^{2+}]2[NTf_2^{-}]$, $[Ni(BnIm)_4^{2+}]2[Cl^{-}]$ and $[Ni(BnIm)_4^{2+}]2[NTf_2^{-}]$) showed the greatest selectivity in extracting the different sized duplex DNA fragments, with

higher EF values obtained for the extraction of ~20 kbp stDNA and ~250-500 bp DNA fragments than the 20 bp DNA fragment.

The *in situ* MIL-DLLME method showed advantages over existing DNA extraction protocols due to its speed (3 min per extraction) and simplicity. Future studies are focused on the application of the in situ MIL-DLLME method to real biological samples as well as designing a MIL-compatible qPCR buffer in order to facilitate direct analysis of extracted DNA from the MIL droplet.

2.6. Acknowledgements

The authors thank Deyny L. Mendivelso-Pérez for performing the Raman spectroscopy measurements and Alan Medina-Gonzalez for performing the X-ray diffraction measurements in this study. J. L. A. acknowledges funding from the Chemical Measurement and Imaging Program at the National Science Foundation (CHE-1709372).

2.7. Compliance with Ethical Standards

2.7.1. Conflicts of Interest

The authors declare that they have no conflict of interest.

2.7.2. Research Involving Human Participants and/or Animals Informed Consent

This article does not contain any studies with human participants or animals performed by any of the authors.

2.8. References

1. Reece JB, Urry LA, Cain ML, Wasserman SA, Minorsky P V., Jackson RB. Campbell Biology, 9th ed. Pearson Education, Inc., San Francisco, CA, USA; 2011.

2. Orr A, Stotesbury T, Wilson P, Stock NL. The use of high-resolution mass spectrometry (HRMS) for the analysis of DNA and other macromolecules: A how-to guide for forensic chemistry. Forensic Chem. 2019;100169(14):1-12. https://doi.org/10.1016/j.forc.2019.100169.

3. Blau S, Catelli L, Garrone F, Hartman D, Romanini C, Romero M, Vullo C. The contributions of anthropology and mitochondrial DNA analysis to the identification of the human skeletal remains of the Australian outlaw Edward “Ned” Kelly. Forensic Sci Int. 2014;240:e11-e21 . https://doi.org/10.1016/j.forsciint.2014.04.009.

4. Li J, Zhou X, Liu X, Ren J, Wang J, Wang W, Zheng Y, Shi X, Sun T, Li Z, Kang A, Tang F, Wen L, Fu W. Detection of Colorectal Cancer in Circulating Cell-Free DNA by Methylated CpG Tandem Amplification and Sequencing. Clin Chem. 2019;65(7):916-926. https://doi.org/10.1373/clinchem.2019.301804.

5. Whitcomb DC, Shelton CA, Brand RE. Genetics and Genetic Testing in Pancreatic Cancer. Gastroenterology. 2015;149(5):1252-1264.e4. https://doi.org/10.1053/j.gastro.2015.07.057.

6. Parsons J, Altmann F, Graf M, Stadlmann J, Reski R, Decker EL. A gene responsible for prolyl-hydroxylation of moss-produced recombinant human erythropoietin. Sci Rep. 2013;3019(3):1-8. https://doi.org/10.1038/srep03019.

7. Tan SC, Yiap BC. DNA, RNA, and Protein Extraction: The Past and The Present. J Biomed Biotechnol. 2009;1-10. https://doi.org/10.1155/2009/574398.

8. Green MR, Sambrook J. Isolation of high-molecular-weight DNA using organic solvents Cold Spring Harb Protoc. 2017;(4):356-59. https://doi.org/10.1101/pdb.prot093450.

9. Abdel-Latif A, Osman G. Comparison of three genomic DNA extraction methods to obtain high DNA quality from maize. Plant Methods. 2017;13:1-9. https://doi.org/10.1186/s13007-016-0152-4.

10. Clark KD, Nacham O, Purslow JA, Pierson SA, Anderson JL. Magnetic ionic liquids in analytical chemistry: A review. Anal Chim Acta. 2016;934:9-21. https://doi.org/10.1016/j.aca.2016.06.011.

11. Clark KD, Emaus MN, Varona M, Bowers AN, Anderson JL. Ionic liquids: solvents and sorbents in sample preparation. J Sep Sci. 2018;41(1):209-35. https://doi.org/10.1002/jssc.201700864.

12. Clark KD, Trujillo-Rodríguez MJ, Anderson JL. Advances in the analysis of biological samples using ionic liquids. Anal Bioanal Chem. 2018;410(19):4567-73. https://doi.org/10.1007/s00216-018-0898-9.

13. Ho TD, Zhang C, Hantao LW, Anderson JL. Ionic Liquids in Analytical Chemistry: Fundamentals, Advances, and Perspectives. Anal Chem. 2014;86(1):262-85. https://doi.org/10.1021/ac4035554.

14. Trujillo-Rodríguez MJ, Nan H, Varona M, Emaus MN, Souza ID, Anderson JL. Advances of Ionic Liquids in Analytical Chemistry. Anal Chem. 2019;91(1):505-31. https://doi.org/10.1021/acs.analchem.8b04710.

15. Sun P, Armstrong DW. Ionic liquids in analytical chemistry. Anal Chim Acta. 2010;661(1):1-16. https://doi: 10.1016/j.aca.2009.12.007.

16. Anderson JL, Armstrong DW, Wei GT. Ionic liquids in analytical chemistry. Anal Chem. 2006;78(9):2893-2902. https://doi.org/10.1021/ac069394o.

17. Trujillo-Rodríguez MJ, Rocío-Bautista P, Pino V, Afonso AM. Ionic liquids in dispersive liquid-liquid microextraction. Trends Anal Chem. 2013;51:87-106. https://doi.org/10.1016/j.trac.2013.06.008.

18. Sajid M. Magnetic ionic liquids in analytical sample preparation: A literature review. Trends Anal Chem. 2019;113:210-223. https://doi.org/10.1016/j.trac.2019.02.007.

19. MacFarlane DR, Kar M, Pringle JM. Fundamentals of Ionic Liquids. Wiley-VCH, Weinheim, Germany; 2017.

20. Li T, Joshi MD, Ronning DR, Anderson JL. Ionic liquids as solvents for in situ dispersive liquid-liquid microextraction of DNA. J Chromatogr A. 2013;1272:8-14. https://doi.org/10.1016/j.chroma.2012.11.055.

21. Clark KD, Nacham O, Yu H, Li T, Yamsek MM, Ronning DR, Anderson JL. Extraction of DNA by magnetic ionic liquids: Tunable solvents for rapid and selective DNA analysis. Anal Chem. 2015;87(3):1552-59. https://doi.org/10.1021/ac504260t.

22. Wang X, Xing L, Shu Y, Chen X, Wang J. Novel polymeric ionic liquid microspheres with high exchange capacity for fast extraction of plasmid DNA. Anal Chim Acta. 2014;837:64-9. https://doi.org/10.1016/j.aca.2014.06.002.

23. Emaus MN, Clark KD, Hinners P, Anderson JL. Preconcentration of DNA using magnetic ionic liquids that are compatible with real-time PCR for rapid nucleic acid quantification. Anal Bioanal Chem. 2018;410(17):4135-44. https://doi.org/10.1007/s00216-018-1092-9.

24. Wang JH, Cheng DH, Chen XW, Du Z, Fang ZL. Direct extraction of double-stranded DNA into ionic liquid 1-butyl-3-methylimidazolium hexafluorophosphate and its quantification. Anal Chem. 2007;79(2):620-5. https://doi.org/10.1021/ac061145c.

25. Peng X, Clark KD, Ding X, Zhu C, Varona M, Emaus MN, An J, Anderson JL. Coupling oligonucleotides possessing a poly-cytosine tag with magnetic ionic liquids for sequence-specific DNA analysis. Chem Commun. 2018;54:10284-7. https://doi.org/10.1039/C8CC05954C.

26. Emaus MN, Varona M, Anderson JL. Sequence-specific preconcentration of a mutation prone KRAS fragment from plasma using ion-tagged oligonucleotides coupled to qPCR compatible magnetic ionic liquid solvents. Anal Chim Acta. 2019;1068:1-10. https://doi.org/10.1016/j.aca.2019.04.005.

27. Marengo A, Cagliero C, Sgorbini B, Anderson JL, Emaus MN, Bicchi C, Bertea CM, Rubiolo P. Development of an innovative and sustainable one-step method for rapid plant DNA isolation for targeted PCR using magnetic ionic liquids. Plant Methods. 2019;15(23):1-11. https://doi.org/10.1186/s13007-019-0408-x.

28. García EG, Ressmann AK, Gaertner P, Zirbs R, Mach RL, Krska R, Bica K, Brunner K. Direct extraction of genomic DNA from maize with aqueous ionic liquid buffer systems for applications in genetically modified organisms analysis. Anal Bioanal Chem. 2014;406(30):7773-84. https://doi.org/10.1007/s00216-014-8204-y.

29. Ressmann AK, García EG, Khlan D, Gaertner P, Mach RL, Krska R, Brunner K, Bica K. Fast and efficient extraction of DNA from meat and meat derived products using aqueous ionic liquid buffer systems. New J Chem. 2015;39:4994-5002. https://doi.org/10.1039/c5nj00178a.

30. Nacham O, Clark KD, Anderson JL. Analysis of bacterial plasmid DNA by solid-phase microextraction. Anal Methods. 2015;7:7202-7. https://doi.org/10.1039/c5ay00532a.

31. Nacham O, Clark KD, Anderson JL. Extraction and Purification of DNA from Complex Biological Sample Matrices Using Solid-Phase Microextraction Coupled with Real-Time PCR. Anal Chem. 2016;88(15):7813-20. https://doi.org/10.1021/acs.analchem.6b01861.

32. Nacham O, Clark KD, Varona M, Anderson JL. Selective and Efficient RNA Analysis by Solid-Phase Microextraction. Anal Chem. 2017;89(20):10661-6. https://doi.org/10.1021/acs.analchem.7b02733.

33. Varona M, Ding X, Clark KD, Anderson JL. Solid-Phase Microextraction of DNA from Mycobacteria in Artificial Sputum Samples to Enable Visual Detection Using Isothermal Amplification. Anal Chem. 2018;90(11):6922-8. https://doi.org/10.1021/acs.analchem.8b01160.

34. Varona M, Anderson JL. Visual Detection of Single-Nucleotide Polymorphisms Using Molecular Beacon Loop-Mediated Isothermal Amplification with Centrifuge-Free DNA Extraction. Anal Chem. 2019;91(11):6991-5. https://doi.org/10.1021/acs.analchem.9b01762.

35. Ventura SPM, E Silva FA, Quental MV, Mondal D, Freire MG, Coutinho JAP. Ionic-Liquid-Mediated Extraction and Separation Processes for Bioactive Compounds: Past, Present, and Future Trends. Chem Rev. 2017;117(10):6984-7052. https://doi.org/10.1021/acs.chemrev.6b00550.

36. Rezaee M, Assadi Y, Milani Hosseini M-R, Aghaee E, Ahmadi F, Berijani S. Determination of organic compounds in water using dispersive liquid–liquid microextraction. J Chromatogr A. 2006;1116(1-2):1-9. https://doi.org/10.1016/j.chroma.2006.03.007.

37. Yu H, Merib J, Anderson JL. Faster dispersive liquid-liquid microextraction methods using magnetic ionic liquids as solvents. J Chromatogr A. 2016;1463:11-19. https://doi.org/10.1016/j.chroma.2016.08.007.

38. An J, Rahn KL, Anderson JL. Headspace single drop microextraction versus dispersive liquid-liquid microextraction using magnetic ionic liquid extraction solvents. Talanta. 2017;167:268-78. https://doi.org/10.1016/j.talanta.2017.01.079.

39. Yao C, Anderson JL. Dispersive liquid-liquid microextraction using an in situ metathesis reaction to form an ionic liquid extraction phase for the preconcentration of aromatic compounds from water. Anal Bioanal Chem. 2009;395:1491-1502. https://doi.org/10.1007/s00216-009-3078-0.

40. Baghdadi M, Shemirani F. In situ solvent formation microextraction based on ionic liquids: A novel sample preparation technique for determination of inorganic species in saline solutions. Anal Chim Acta. 2009;634(2):186-91. https://doi.org/10.1016/j.aca.2008.12.017.

41. Chand D, Farooq MQ, Pathak AK, Li J, Smith EA, Anderson JL. Magnetic ionic liquids based on transition metal complexes with N-alkylimidazole ligands. New J Chem. 2019;43:20-3. https://doi.org/10.1039/C8NJ05176C.

42. Trujillo-Rodríguez MJ, Anderson JL. In situ formation of hydrophobic magnetic ionic liquids for dispersive liquid-liquid microextraction. J Chromatogr A. 2019;1588:8-16. https://doi.org/10.1016/j.chroma.2018.12.032.

43. Trujillo-Rodríguez MJ, Anderson JL. In situ generation of hydrophobic magnetic ionic liquids in stir bar dispersive liquid-liquid microextraction coupled with headspace gas chromatography. Talanta. 2019;196:420-8. https://doi.org/10.1016/j.talanta.2018.12.071.

44. Miura Y, Shimizu F, Mochida T. Preparation, properties, and crystal structures of organometallic ionic liquids comprising 1-ferrocenyl-3-alkylimidazolium-based salts of bis(trifluoromethanesulfonyl)amide and hexafluorophosphate. Inorg Chem. 2010;49(21):10032-40. https://doi.org/10.1021/ic1013363.

45. Del Sesto RE, Corley C, Robertson A, Wilkes JS. Tetraalkylphosphonium-based ionic liquids. J Organomet Chem. 2005;690(10):2536-42. https://doi.org/10.1016/j.jorganchem.2004.09.060.

46. Santos E, Albo J, Rosatella A, Afonso CAM, Irabien Á. Synthesis and characterization of Magnetic Ionic Liquids (MILs) for CO2 separation. J Chem Technol Biotechnol. 2014;89:866-71. https://doi.org/10.1002/jctb.4323.

47. Pierson SA, Nacham O, Clark KD, Nan H, Mudryk Y, Anderson JL. Synthesis and characterization of low viscosity hexafluoroacetylacetonate-based hydrophobic magnetic ionic liquids. New J Chem. 2017;41:5498-5505. https://doi.org/10.1039/c7nj00206h.

48. Weller M, Overton T, Rourke J, Armstrong F. Inorganic Chemistry, 6th ed. Oxford: University Press; 2014.

49. Kapinos LE, Song B, Sigel H. Metal-ion coordinating properties of imidazole and derivatives in aqueous solution: interrelation between complex stability and ligand basicity. Inorganica Chim Acta. 1998;280(1-2):50-6. https://doi.org/10.1016/S0020-1693(98)00052-8.

50. Khiat M, Pacheco-Fernández I, Pino V, Benabdallah T, Ayala JH, Afonso AM. A guanidinium ionic liquid-based surfactant as an adequate solvent to separate and preconcentrate cadmium and copper in water using in situ dispersive liquid-liquid microextraction. Anal Methods. 2018;10:1529-37. https://doi.org/10.1039/c8ay00022k.

51. Anastassopoulou J. Metal-DNA interactions. J Mol Struct. 2003;651-653:19-26. https://doi.org/10.1016/S0022-2860(02)00625-7.

52. Leonarski F, D'Ascenzo L, Auffinger P. Binding of metals to purine N7 nitrogen atoms and implications for nucleic acids: A CSD survey. Inorganica Chim Acta. 2016;452:82-9 . https://doi.org/10.1016/j.ica.2016.04.005.

53. Tateishi-Karimata H, Sugimoto N. Biological and nanotechnological applications using interactions between ionic liquids and nucleic acids. Biophys Rev. 2018;10(3):931-40. https://doi.org/10.1007/s12551-018-0422-7.

54. Chandran A, Ghoshdastidar D, Senapati S. Groove binding mechanism of ionic liquids: A key factor in long-term stability of DNA in hydrated ionic liquids? J Am Chem Soc. 2012;134(50):20330-9. https://doi.org/10.1021/ja304519d.

55. Ding X, Clark KD, Varona M, Emaus MN, Anderson JL. Magnetic ionic liquid-enhanced isothermal nucleic acid amplification and its application to rapid visual DNA analysis. Anal Chim Acta. 2019;1045:132-140. https://doi.org/10.1016/j.aca.2018.09.014.

56. Ennis E, Handy ST. A facile route to C2-substituted imidazolium ionic liquids. Molecules. 2009;14(6):2235-45. https://doi.org/10.3390/molecules14062235.

CHAPTER 3. FLUORESCENCE QUENCHING OF THE SYBR GREEN I-dsDNA COMPLEX BY IN SITU MAGNETIC IONIC LIQUIDS

Ashley N. Bowers, Kalyan Santra, María J. Trujillo-Rodríguez, Anthony Song, Jacob W. Petrich, and Jared L. Anderson

Department of Chemistry, Iowa State University, Ames, Iowa 50011 USA

Modified from a manuscript to be submitted to Journal of Physical Chemistry

3.1. Abstract

Magnetic ionic liquids (MILs) with metal-containing cations are promising extraction solvents that provide fast and high efficiency extraction of DNA through the *in situ* generation of a hydrophobic MIL-microdroplet in a methodology called *in situ* dispersive liquid-liquid microextraction. To consolidate the sample preparation workflow, it is desirable to directly use the DNA enriched MIL-microdroplet in the subsequent analytical detection technique. Fluorescence-based techniques employed for DNA detection, oftentimes use SYBR Green I, a DNA binding dye which exhibits optimal fluorescence when bound to double-stranded DNA. However, the presence of a metal in the cation or anion of the MIL structure may hinder the fluorescence signal of this complex due to quenching. In this study, the fluorescence quenching effects of the aforementioned new generation of MILs using a SYBR Green I dye-double stranded DNA complex were evaluated using Förster Resonance Energy Transfer and quantified using Stern-Volmer models. The studied MILs were based on N-substituted imidazole ligands (with butyl- and benzyl- groups as substituents) coordinated to Ni^{2+} or Co^{2+} metal centers as cations, and chloride anions. The quenching effect of $NiCl_2$ and $CoCl_2$ salts and the 1-butyl-3-methylimidazolium chloride ionic liquid on the fluorophore complex was also studied to understand the components of the MIL structure that are responsible for quenching. The metal of the MIL was found to be the main component in their structure contributing to fluorescence

quenching. Förster critical distances between 11.9 and 18.8 Å were obtained for the MILs, indicating that quenching is likely not due to non-radiative energy transfer but rather through spin-orbit coupling or excited-state electron transfer.

Keywords: DNA; *in situ* magnetic ionic liquids; fluorescence spectroscopy; fluorescence quenching; fluorescence resonance energy transfer; Stern-Volmer relationship

3.2. Introduction

DNA analysis is central to many applications in clinical diagnostics,[1] personalized medicine,[2] forensics,[3] and archaeology.[4] The majority of DNA analysis methodologies use polymerase chain reaction (PCR)[5] and fluorescence-based assays.[6] In quantitative PCR (qPCR), the amplified DNA binds to a fluorescent dye, such as SYBR Green I, and the amount of amplified DNA can be monitored in real-time by the increase in the fluorescent signal of the dye-DNA fluorophore complex.[7]

For performing both PCR and fluorescence-based DNA analysis, sample pretreatment steps are generally required to extract and purify DNA from the biological matrix. Small amounts of contaminating species (such as other nucleic acids, proteins, etc.) and the quality of the DNA obtained can affect the reliability of the results.[8,9] Traditional DNA extraction protocols use large amounts of toxic solvents and/or sorbents[8] and often involve numerous steps resulting in variable amounts of recovered DNA.[10]

As an alternative to the aforementioned traditional methods, ionic liquids (ILs) and, more recently, magnetic ionic liquids (MILs) have been increasingly used as greener solvents for the extraction and preservation of nucleic acids.[11-17] ILs are molten salts composed solely of ions and exhibit melting points below 100 ºC and tunable physical and chemical properties.[18] MILs are a subclass of ILs that contain a paramagnetic component in their cationic and/or anionic moiety and respond to an applied magnetic field.[19-22] MILs possess many of the same advantageous

properties of ILs such as low vapor pressure at room temperature, variable viscosity and solubility in water or organic solvents, unique solvation capabilities for both hydrophilic and hydrophobic compounds, and electrical conductivity.[23] As a result of these characteristics, both IL and MIL-based extraction methods provide high extraction efficiencies for DNA. In addition, MILs have the ability to be collected with a strong external magnet, replacing time-consuming centrifugation steps.

The majority MILs employed in DNA extractions contained the paramagnetic component in the anion.[13,15] However, in a recent report, MILs possessing paramagnetic cations and chloride anions were investigated for the extraction of DNA.[24] This class of MILs, initially soluble in aqueous solution, were able to undergo a metathesis reaction during the extraction to generate a hydrophobic MIL *in situ*, facilitating the rapid extraction of DNA. These MILs extracted 20 bp DNA, ~250-500 bp DNA and ~20 kbp DNA with high extraction efficiencies (>42%) using *in situ* dispersive liquid-liquid microextraction in combination to indirect detection methods.[24]

When MIL-based DNA extractions are directly combined to PCR, customized PCR buffers are generally designed to alleviate the PCR inhibition caused by cationic and anionic components of the MIL.[15,25] Despite the use of these buffers, quantitative PCR was not possible in the case of MILs containing Fe(III)-anions due to quenching of the fluorescence signal.[26] To deeply understand the behavior of MILs and their structural components in fluorescence-based applications, fluorescence quenching mechanisms can be examined using Förster Resonance Energy Transfer (FRET) or quantified using Stern-Volmer models.[26] FRET evaluates the non-radiative energy transfer from a fluorescent donor to a ground-state acceptor as defined by the overlap integral.[26,27] Stern-Volmer plots represent the fluorescence signal when increasing concentration of quencher is added and constitute a method commonly used to determine the

magnitude and nature of fluorescence quenching.[26,28,29] In a previously published study, both FRET and Stern-Volmer models were applied to MILs containing phosphonium cations and paramagnetic anion complexes in which different metals were coordinated with chloride or hexafluoroacetylacetonate (hfacac) ligands. Cyanine5 carboxylic acid (Cy5) was employed as the fluorophore in this study, which is fluorescent in its native form and when tagged to DNA. The authors found that Fe(III)- and Co(II)-based MILs strongly quenched the fluorescence signal.[26] However, quenching was much less pronounced with MILs containing Mn(II) and were deemed to be more compatible for direct use in fluorescence-based assays.[26] Other paramagnetic metal complexes have also been shown to quench fluorescence signals in different studies.[30,31] With regards to the use of MILs containing paramagnetic cations, no studies on their fluorescence quenching effects have been explored yet.

In this study, fluorescence quenching of the SYBR Green I-double-stranded DNA (dsDNA) complex by the aforementioned new generation of MILs containing paramagnetic cations was investigated. The MILs studied contained four N-substituted imidazole ligands (N-butylimidazole or N-benzylimidazole) coordinated to Ni^{2+} or Co^{2+} metal centers and chloride anions. The use of the selected fluorophore complex (SYBR Green I-dsDNA) provided an environment similar to fluorescence-based DNA detection methods. FRET and fluorescence quenching studies using Stern-Volmer models were performed to evaluate the quenching effects of the MILs in the system. $NiCl_2$, $CoCl_2$ metal salts and the 1-butyl-3-methylimidazolium chloride ($[BMIm^+][Cl^-]$) IL were employed as controls to better understand the components of the MIL structure that are responsible for quenching.

3.3. Experimental

3.3.1. Chemicals, Reagents, Materials

Double-stranded DNA (dsDNA; ~20 kbp salmon testes DNA) used in this study was purchased from Sigma-Aldrich (St. Louis, MO, USA). SYBR Green I (10,000×) was purchased from Life Technologies (Eugene, OR, USA). Tris(hydroxymethyl)aminomethane (Tris base) was purchased from Research Products International (Mount Prospect, IL, USA). Ultrapure water (18.2 MΩ·cm) was obtained from a Milli-Q water purification system (Millipore, Bedford, MA, USA). Disposable cuvettes made of poly(methyl methacrylate) (PMMA) and hydrochloric acid (ACS grade, 36.5-38.0%) were purchased from Fisher Scientific (Fair Lawn, NJ, USA).

For the synthesis of the IL and MILs, the reagents cobalt(II) chloride (97%), 1-butylimidazole (98%), 1-chlorobutane (99%), 1-methylimidazole (99%) as well as HPLC-grade ethyl acetate were purchased from Sigma-Aldrich. Nickel(II) chloride (98%) and benzylimidazole (99%) were purchased from Acros Organics (Morris Plains, NJ, USA). Anhydrous diethyl ether (99.0%) was purchased from Avantor Performance Materials Inc. (Center Valley, PA, USA). Deuterated dimethyl sulfoxide-d6 (DMSO-*d6*, 99.9%) was purchased from Cambridge Isotope Laboratories (Andover, MA, USA).

Chemical structures of the IL, MILs and SYBR Green I dye used in this study are shown in Figure 1. Stock solutions of the MILs, IL and metal salts were prepared in 10 mM Tris-HCl buffer (pH 8) at the following concentrations: 10 mM, 1 mM and 0.1 mM for $NiCl_2$, $CoCl_2$, tetra(benzylimidazole)nickel (II) chloride ($[Ni(BnIm)_4^{2+}]2[Cl^-]$) and tetra(butylimidazole)cobalt (II) chloride ($[Co(BIm)_4^{2+}]2[Cl^-]$), 16 mM, 1 mM and 0.1 mM for tetra(butylimidazole)nickel (II) chloride ($[Ni(BIm)_4^{2+}]2[Cl^-]$) and 110 mM, 10 mM and 1 mM for $[BMIm^+][Cl^-]$. Stock solutions of the dsDNA and SYBR Green I were also prepared in Tris-HCl buffer at concentrations of 154 nM and 98 µM, respectively.

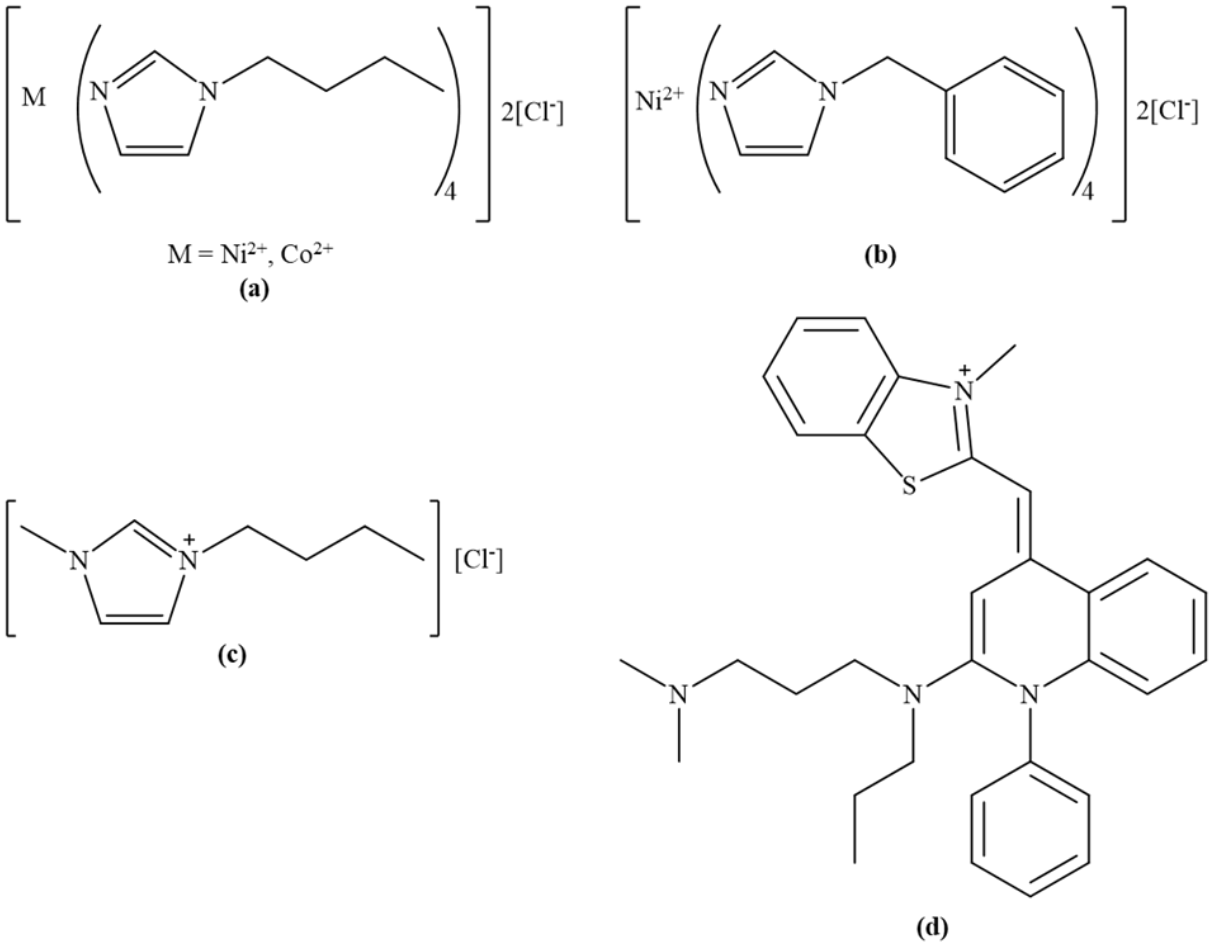

Figure 1. Chemical structures of the MILs, IL and fluorophore used in this study. **(a)** $[Ni(BIm)_4^{2+}]2[Cl^-]$ and $[Co(BIm)_4^{2+}]2[Cl^-]$, **(b)** $[Ni(BnIm)_4^{2+}]2[Cl^-]$ **(c)** $[BMIm^+][Cl^-]$ and **(d)** SYBR Green I.

3.3.2. Instrumentation and Methods

Steady-state absorption and fluorescence spectra were obtained using an Agilent Technologies 8453 UV-visible spectrophotometer and an Agilent Cary Eclipse fluorescence spectrophotometer (Santa Clara, CA, USA), respectively. Emission spectra were obtained with 1-nm resolution and corrected for lamp spectral intensity and detector response. The excitation and emission slit widths were 5 nm and the photomultiplier (PMT) detector voltage was 550 V.

The samples were excited at 475 nm with the emission intensity recorded from 485 nm to 700 nm.

$[BMIm^+][Cl^-]$ was synthesized and purified following a previously reported procedure.[32] The final product was characterized by ^{1}H-NMR, with the spectra recorded in DMSO-*d6* using a Bruker DRX 500 MHz nuclear magnetic resonance (NMR) spectrometer (Billerica MA, USA) (see Figure B1 of Appendix B). The MILs were synthesized and purified using previously reported methods.[33]

Samples for fluorescence quenching experiments were prepared in 1-cm path length PMMA cuvettes. All samples were prepared in 10 mM Tris-HCl buffer (pH 8) and the total volume, dsDNA concentration, and SYBR Green I concentration were kept constant at 2 mL, 1 nM and 1.96 µM, respectively. Stock solutions referred to in Section 2.1 were used to prepare the samples and were prepared in triplicate the same day as the experiment by mixing for 15 s using a vortex (Fisher Scientific). The exception was the dsDNA stock solution, which was stored in 10 mM Tris-HCl buffer at 4 ^{o}C. The samples were prepared over a range of increasing concentration of the quenchers ($NiCl_2$, $CoCl_2$, $[Ni(BIm)_4^{2+}]2[Cl^-]$, $[Co(BIm)_4^{2+}]2[Cl^-]$ or $[BMIm^+][Cl^-]$). The concentration of the $NiCl_2$ and $CoCl_2$ salts ranged from 0 to 0.5 mM. The concentration of the $[Ni(BIm)_4^{2+}]2[Cl^-]$ and $[Ni(BnIm)_4^{2+}]2[Cl^-]$ MILs varied from 0 to 1 mM. The $[Co(BIm)_4^{2+}]2[Cl^-]$ MIL concentration ranged from 0 to 0.1 mM and the concentration of the $[BMIm^+][Cl^-]$ IL from 0 to 100 mM.

3.4. Results and Discussion

3.4.1. Quantifying Fluorescence Quenching of the SYBR Green I-DNA Complex

Fluorescence quenching can be induced by a variety of molecular interactions such as excited-state reactions, complex-formation, energy transfer and collisional quenching.[28] Collisional (or sometimes called dynamic) quenching occurs as a result of collisions between an

excited-state fluorophore and quencher molecules.[34] On the other hand, a reaction between the quencher in the ground-state and the fluorophore resulting in ground-state complex formation is defined as static quenching.[34] These types of quenching are commonly described by Stern-Volmer equations.[28,35-37] Collisional quenching or static quenching is described by Eq. (1):

$$\frac{F_0}{F} = 1 + K_{SV}[Q] \qquad \text{Eq. (1)}$$

where F_0 is the integrated fluorescence intensity of the corrected spectra when the concentration of quencher is 0, F is the integrated fluorescence intensity of the corrected spectra when the concentration of the quencher is $[Q]$ and K_{SV} is the Stern-Volmer quenching constant. If the Stern-Volmer plot of F_0/F versus $[Q]$ is linear, the Stern-Volmer quenching constant can be extrapolated from the slope with a "y-intercept" of 1. In general, a single class of fluorophores displays a linear Stern-Volmer plot, all of which have equal accessibility to the quencher.

A deviation from linearity towards the "x-axis" is evident from a Stern-Volmer plot of F_0/F *versus* $[Q]$ when at least one of two (or more) populations of fluorophores are accessible to the quencher. These two populations can have different accessibilities to the quencher, with one fraction being accessible, *a*, and the other fraction buried, *b*, thus is inaccessible. The total fluorescence in absence of the quencher, F_0, is equal to the fluorescence intensity of the two fractions, *a* and *b*, in absence of the quencher, Eq. (2)[28,35,38]:

$$F_0 = F_{0a} + F_{0b} \qquad \text{Eq. (2)}$$

This type of quenching is described by a modified form of the Stern-Volmer equation, Eq. (3)[25,35,38]:

$$\frac{F_0}{F_0 - F} = \frac{1}{f_a K_a [Q]} + \frac{1}{f_a} \qquad \text{Eq. (3)}$$

where F_0 and F are the integrated fluorescence intensities of the corrected spectra when the concentration of the quencher is 0 and *[Q]*, respectively. K_a is the Stern-Volmer quenching constant of the accessible fraction and f_a is the accessible fraction of fluorescence available to the quencher. K_a and f_a can be determined from a plot of $F_0/(F_0-F)$ *versus* $1/[Q]$, which should be linear, with f_a^{-1} as the "y-intercept" and $(f_aK_a)^{-1}$ as the slope.

For quantifying fluorescence quenching of the SYBR Green I-dsDNA complex, Stern-Volmer plots of the complex quenched by the $NiCl_2$, $CoCl_2$, $[Ni(BIm)_4^{2+}]2[Cl^-]$, $[Ni(BnIm)_4^{2+}]2[Cl^-]$ and $[Co(BIm)_4^{2+}]2[Cl^-]$ MILs were constructed. The obtained plots are presented in Figures 2-4 and B4-B5 of Appendix B. The plots fit to the modified Stern-Volmer equation, Eq. (3), curving downward toward the "x-axis" at increasing concentrations of quencher. These results will be detailed in the following sections.

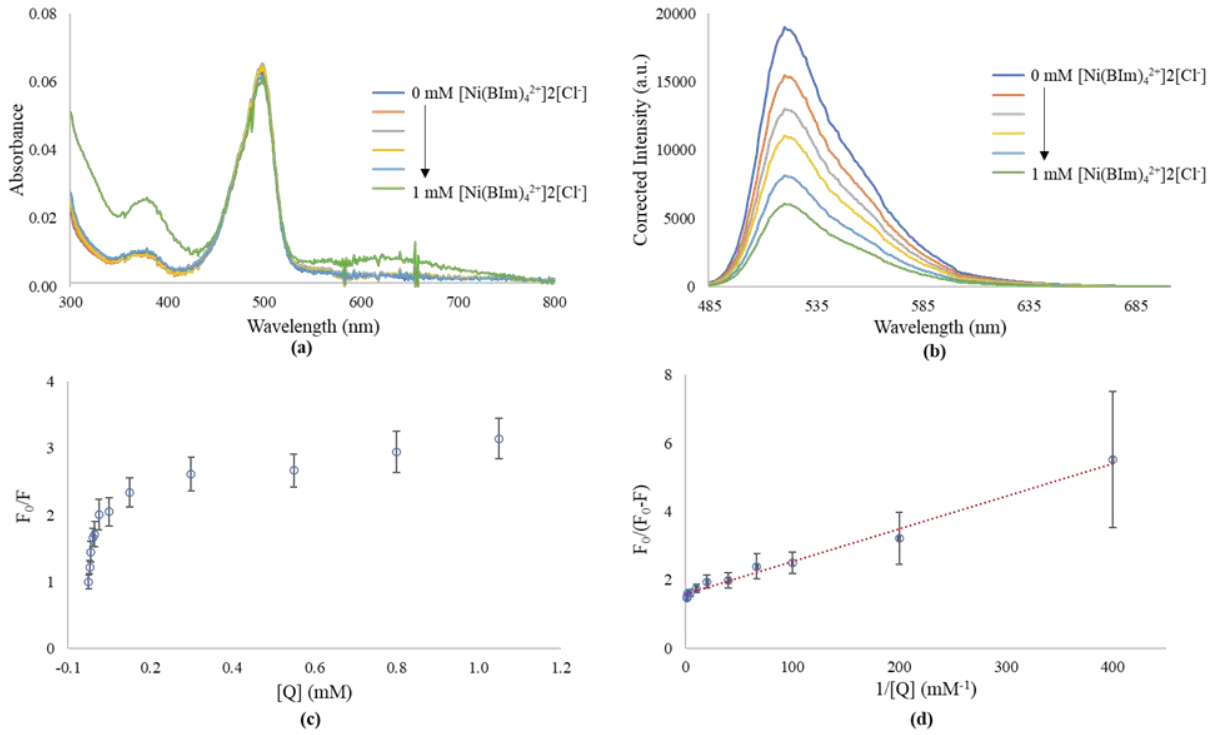

Figure 2. Fluorescence quenching of the SYBR Green I-dsDNA complex as a function of $[Ni(BIm)_4^{2+}]2[Cl^-]$ concentration. **(a)** Absorption spectra. **(b)** Fluorescence emission spectra, λ_{ex} = 475 nm. Intensities were corrected for the absorption at the wavelength of excitation. **(c)** Steady-state Stern-Volmer plot of the integrate fluorescence intensity ratio (F_0/F) as a function

of quencher concentration. **(d)** Steady-state modified Stern-Volmer plot of the integrated fluorescence intensity ratio ($F_0/(F_0-F)$) and as a function of *1/[Q]*.

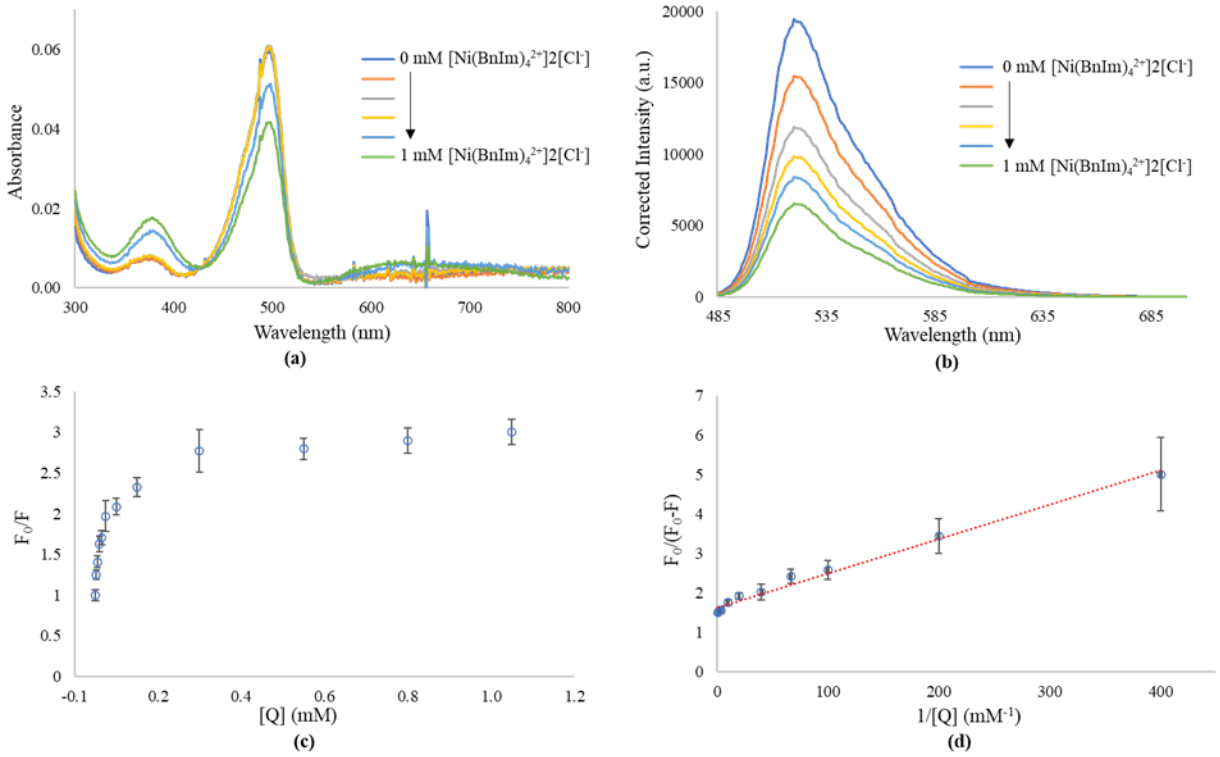

Figure 3. Fluorescence quenching of the SYBR Green I-dsDNA complex as a function of $[Ni(BnIm)_4^{2+}]2[Cl^-]$ concentration. **(a)** Absorption spectra. **(b)** Fluorescence emission spectra, λ_{ex} = 475 nm. Intensities were corrected for the absorption at the wavelength of excitation. **(c)** Steady-state Stern-Volmer plot of the integrate fluorescence intensity ratio (F_0/F) as a function of quencher concentration. **(d)** Steady-state modified Stern-Volmer plot of the integrated fluorescence intensity ratio ($F_0/(F_0-F)$) and as a function of *1/[Q]*.

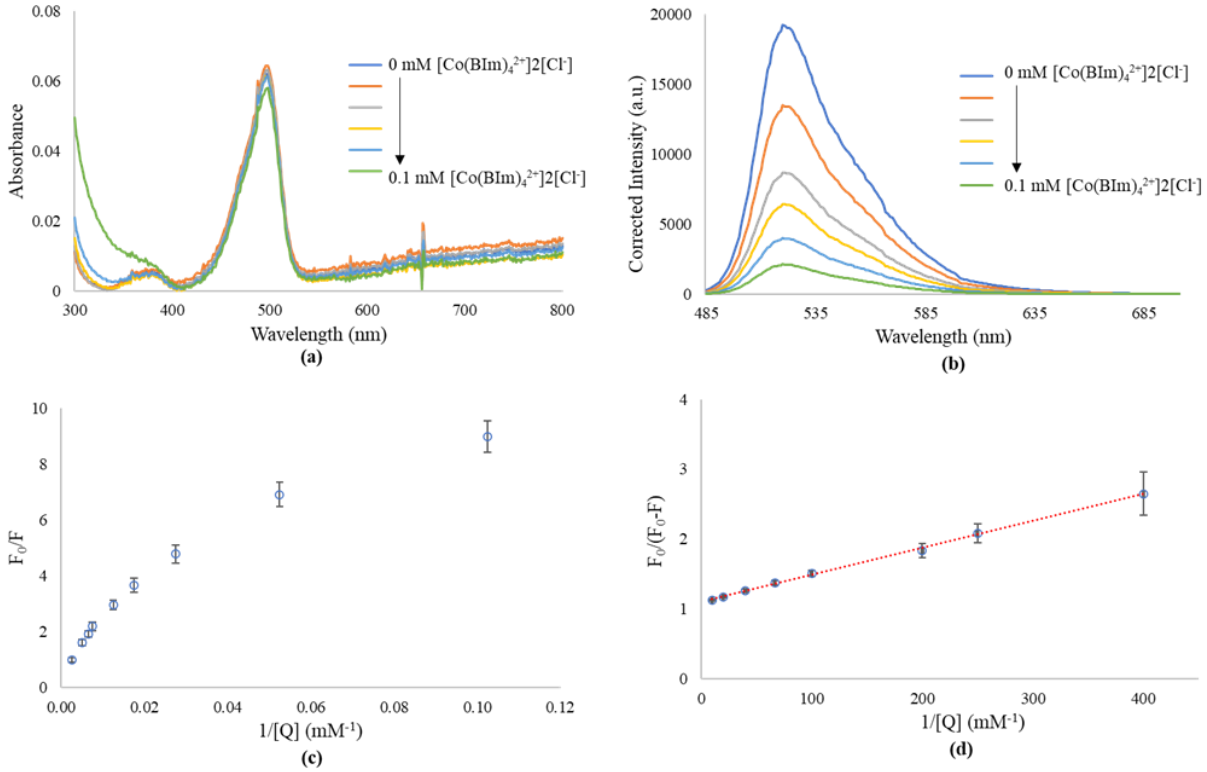

Figure 4. Fluorescence quenching of the SYBR Green I-dsDNA complex as a function of $[Co(BIm)_4^{2+}]2[Cl^-]$ concentration. **(a)** Absorption spectra. **(b)** Fluorescence emission spectra, λ_{ex} = 475 nm. Intensities were corrected for the absorption at the wavelength of excitation. **(c)** Steady-state Stern-Volmer plot of the integrate fluorescence intensity ratio (F_0/F) as a function of quencher concentration. **(d)** Steady-state modified Stern-Volmer plot of the integrated fluorescence intensity ratio ($F_0/(F_0-F)$) and as a function of *1/[Q]*.

3.4.2. Evaluation of the Contribution of Förster Resonance Energy Transfer (FRET) to Fluorescence Quenching

The rate of non-radiative energy transfer, k_T, from a donor to an acceptor was defined by Förster by means of Eq. (4)[4,5,17]:

$$k_T = \frac{1}{\tau_D}\left(\frac{R_0}{R}\right)^6 \qquad \text{Eq. (4)}$$

where R is the distance between the donor and acceptor molecules, τ_D is the fluorescence lifetime of the donor and R_0 is the Förster critical transfer distance, defined by Eq. (5):

$$R_0^6 = \frac{9000 \ln(10) \phi_D \kappa^2}{128 \pi^5 n^4 N_A} \int_0^\infty \frac{F_D(\tilde{\nu}) \varepsilon_A(\tilde{\nu})}{\tilde{\nu}^4} d\tilde{\nu} \qquad \text{Eq. (5)}$$

where ϕ_D is the quantum yield of donor fluorescence emission, κ^2 is the orientation factor and is equal to 2/3 for randomly oriented molecules, n is the solvent refractive index, N_A is Avogadro's number, $F_D(\tilde{\nu})$ is the donor fluorescence emission intensity normalized to unit area on a wavenumber scale, and $\varepsilon_A(\tilde{\nu})$ is the molar decadic extinction coefficient at wavenumber, $\tilde{\nu}$. Non-radiative energy transfer can be determined by the overlap integral of the fluorescence emission spectrum of the donor and the absorbance spectrum of the acceptor, which is evaluated using R_0.

As representative examples, the overlap of the fluorescence emission spectrum of the SYBR Green I-dsDNA complex and the absorbance spectrum of $NiCl_2$, $CoCl_2$, $[Ni(BIm)_4^{2+}]2[Cl^-]$, $[Ni(BnIm)_4^{2+}]2[Cl^-]$ and $[Co(BIm)_4^{2+}]2[Cl^-]$ are shown in Figure B2 of Appendix B, whereas the obtained R_0 values are shown in Table 1. The R_0 values obtained for the metal salts and the MILs were between 9.00-18.8 Å. When compared to the previous generation of MILs containing phosphonium cations and metal chloride or metal hfacac-based anions with Cy5 as the fluorescent donor, R_0 values ranging from 14.2 to 58.1 Å were obtained for the metal salts and the MILs. Out of the studied quenchers, the highest overlap integral was observed for the Co(II) salt (with Cl^- added to achieve a tetrahedral geometry around the metal), which indicated a significant contribution of fluorescence quenching through non-radiative energy transfer was possible. In the current study, R_0 values less than 20 Å were obtained for all of the metal salts and MILs, which does not suggest that non-radiative energy transfer is an important process in the fluorescence quenching of the SYBR Green I-dsDNA complex. Therefore, the ability of the metal salts and this new generation of MILs to quench the fluorescence of SYBR Green I-dsDNA must be through spin-orbit coupling or excited-state electron transfer. However, our current work cannot distinguish between the two mechanisms, as

it is beyond the focus of our investigation. It was still attainable to evaluate the effect of the metal salts and MILs on the SYBR Green I-dsDNA complex through fluorescence quenching studies, as is performed in the following Sections, 3.3.1 and 3.3.2, where increasing concentrations of the metal salts and MILs were added.

Table 1. Förster critical distances (R_0) of the metal salts and MILs obtained using Eq. (5).

Quencher	**R_0 (Å)**
$NiCl_2$	9.00
$CoCl_2$	14.1
$[Ni(BIm)_4^{2+}]2[Cl^-]$	11.9
$[Ni(BnIm)_4^{2+}]2[Cl^-]$	13.9
$[Co(BIm)_4^{2+}]2[Cl^-]$	18.8

3.4.3. Fluorescence Quenching of the SYBR Green I-DNA Complex by the MILs

As previously mentioned, Figures 2-4 show the steady-state Stern-Volmer plots and modified Stern-Volmer plots for the fluorescence quenching of the SYBR Green I-dsDNA complex by the $[Ni(BIm)_4^{2+}]2[Cl^-]$, $[Ni(BnIm)_4^{2+}]2[Cl^-]$ and $[Co(BIm)_4^{2+}]2[Cl^-]$ MILs. The modified Stern-Volmer plots were fit to Eq. (3) and the quenching parameters are presented in Table 2. From the intercept, a value of 0.65 ± 0.01 was obtained for f_a for the two Ni(II)-based MILs, $[Ni(BIm)_4^{2+}]2[Cl^-]$ and $[Ni(BnIm)_4^{2+}]2[Cl^-]$. This result indicates that approximately 65% of the SYBR Green I-dsDNA complex was accessible for quenching by the Ni(II)-based MILs and the other 35% was not affected by the MILs added in the concentration range from 0-1 mM (Figures 2-3). On the other hand, the intercept of the modified Stern-Volmer plot for the $[Co(BIm)_4^{2+}]2[Cl^-]$ MIL yielded a f_a value of 0.92 ± 0.01, meaning that the majority of the

SYBR Green I-dsDNA complex was available to the $[Co(BIm)_4^{2+}]2[Cl^-]$ MIL quencher over the concentration range of 0-0.1 mM. As described in Section 3.4.1., the quenching constants of the accessible fraction, K_a, were 143 ± 20, 137 ± 20, and 265 ± 10 for the $[Ni(BIm)_4^{2+}]2[Cl^-]$, $[Ni(BnIm)_4^{2+}]2[Cl^-]$, and $[Co(BIm)_4^{2+}]2[Cl^-]$ MILs, respectively (see Table 2).

Table 2. The fraction of fluorescence accessible to the quencher (f_a) and the Stern-Volmer quenching constant of the accessible fraction (K_a) for the metal salts and MILs obtained using Eq. (3).

Quencher	**f_a**	**K_a (mM^{-1})**
$NiCl_2$	0.61 ± 0.01	160 ± 10
$CoCl_2$	0.93 ± 0.01	181 ± 10
$[Ni(BIm)_4^{2+}]2[Cl^-]$	0.65 ± 0.01	143 ± 20
$[Ni(BnIm)_4^{2+}]2[Cl^-]$	0.65 ± 0.01	137 ± 20
$[Co(BIm)_4^{2+}]2[Cl^-]$	0.92 ± 0.01	265 ± 10

With regards to the two studied Ni(II)-based MILs ($[Ni(BIm)_4^{2+}]2[Cl^-]$ and $[Ni(BnIm)_4^{2+}]2[Cl^-]$), the f_a and K_a values can be considered equal within experimental error (see Table 2). However, a change in the absorption spectrum of the SYBR Green I-dsDNA complex as higher concentrations of the $[Ni(BnIm)_4^{2+}]2[Cl^-]$ MIL were added was observed, as shown in Figure 3. This possibly indicates quenching due to a static component from complex formation between the SYBR Green I-dsDNA complex and the $[Ni(BnIm)_4^{2+}]2[Cl^-]$ MIL. The BnIm ligand of the MIL can interact with dsDNA through π- π stacking interactions, forming a non-fluorescent ground-state complex, indicative of static quenching.[28,40]

In order to ensure that all of the SYBR Green I dye was bound to dsDNA and that the two populations of fluorophores observed were not from quencher molecules interacting with excess of SYBR Green I, the fluorescence intensity of 1.96 µM SYBR Green I with 1 nM, 3.5

nM and 10 nM of dsDNA (in absence of any quencher) was recorded (Figure B3 of Appendix B). A student's t-test concluded that the integrated fluorescence intensities of the corrected spectra for 1.96 μM SYBR Green I with 1 nM dsDNA compared to the 3.5 nM and 10 nM dsDNA were not statistically different (see Table B1 of Appendix B). This result indicates that all of the SYBR Green I dye in solution is bound to the dsDNA, and that the two populations of fluorophores observed in the quenching experiments were from two different populations of the SYBR Green I-dsDNA complex accessible to the quencher molecules. Thus, 1 nM dsDNA was used for all quenching experiments.

3.4.4. Fluorescence Quenching of the SYBR Green I-DNA Complex by the Metal Salts

To identify the component of the MILs responsible for the quenching of the SYBR Green I-dsDNA complex, Stern-Volmer plots were generated using the $NiCl_2$ and $CoCl_2$ as quenchers (Figures B4 and B5 of Appendix B). The Stern-Volmer plots of the metal chloride salts exhibited the same deviation from linearity towards the "x-axis" as the Stern-Volmer plots of the MILs and, therefore, they were also fit using Eq (3). If the quenching parameters of the MILs and the metal salts are compared, $NiCl_2$ was found to have similar f_a and K_a values as the $[Ni(BIm)_4^{2+}]2[Cl^-]$ and $[Ni(BnIm)_4^{2+}]2[Cl^-]$ MILs, within experimental error (see Table 2). This indicates that $NiCl_2$ and the $[Ni(BIm)_4^{2+}]2[Cl^-]$ and $[Ni(BnIm)_4^{2+}]2[Cl^-]$ MILs have roughly the same quenching effect on the fluorescence of the SYBR Green I-dsDNA complex.

On the other hand, the quenching effect of the $CoCl_2$ was less significant than the $[Co(BIm)_4^{2+}]2[Cl^-]$ MIL, as indicated by the larger K_a value for $[Co(BIm)_4^{2+}]2[Cl^-]$ (see Table 2). However, both the $CoCl_2$ and the Co(II)-based MIL were characterized by a similar f_a value (Table 2). As explained in Section 3.2., the R_0 values of the metal salts and MILs were all found to be below 20 Å, therefore FRET is likely not a main contributor to the quenching effect and the mechanism of quenching must either be through spin-orbit coupling or excited-state electron

transfer. There could be a difference in quenching depending on the geometry of the MIL in solution although this also lies beyond the scope of the current study and was not investigated in further detail.

3.4.5. Effect of the IL (No Metal) Control on the Fluorescence of the SYBR Green I-DNA Complex

To study the effect of a non-magnetic IL on the fluorescence of the SYBR Green I-dsDNA complex, Stern-Volmer plots were obtained by adding 0-100 mM of $[BMIm^+][Cl^-]$ to the SYBR Green I-dsDNA complex. As shown in Figure 5, the Stern-Volmer plot was linear and fit to Eq. (1), yielding a K_{SV} of 1.2 ± 0.2 M^{-1}. This indicates that the $[BMIm^+][Cl^-]$ IL has a negligible effect on the fluorescence of the SYBR Green I-dsDNA complex, and that the metal ions in the cation of the MIL structure are mainly responsible for the fluorescence quenching of the complex.

3.5. Conclusions

In this study, MILs containing the paramagnetic component in the cation and chloride anions were used in absorption and fluorescence emission spectroscopy to evaluate their suitability for use in fluorescence-based DNA applications. The SYBR Green I-dsDNA complex was used as the fluorophore in the assessment of the fluorescence quenching effects of the MILs themselves, and metal chloride salts and a non-magnetic IL for comparison.

As predicted and confirmed through fluorescence quenching experiments, the metal (Co^{2+} or Ni^{2+}) of the MIL was the main component in their structure responsible for quenching

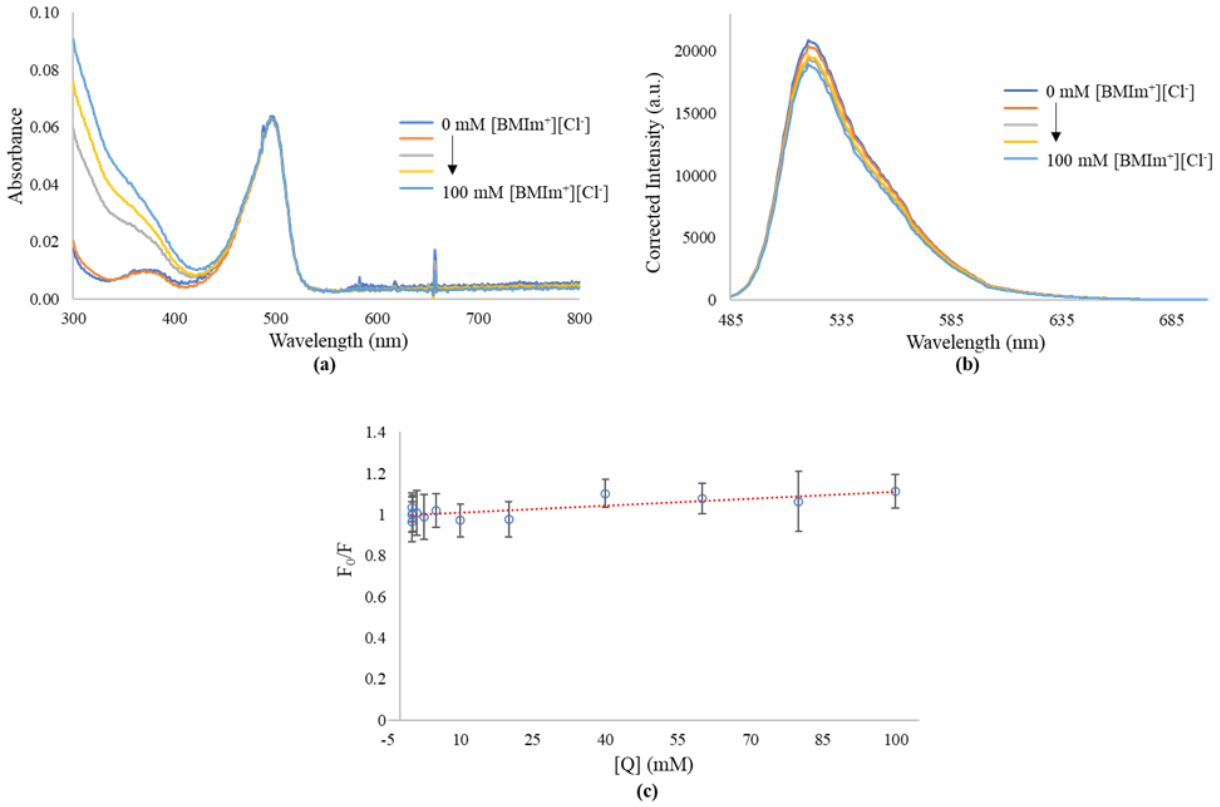

Figure 5. Fluorescence quenching of the SYBR Green I-dsDNA complex as a function of [$BMIm^+$][Cl^-] concentration. **(a)** Absorption spectra. **(b)** Fluorescence emission spectra, $\lambda_{ex} = 475$ nm. Intensities were corrected for the absorption at the wavelength of excitation. **(c)** Steady-state Stern-Volmer plot of the integrate fluorescence intensity ratio (F_0/F) as a function of quencher concentration.

of the fluorescence signal. As increasing concentration of quencher was added, it was found that the SYBR Green I-dsDNA complex provided an environment where two populations of fluorophores were present, both with different accessibilities to the quencher. This behavior was observed for all the MILs and the metal chloride salts. This new generation of MILs exhibited the large quenching constants, as observed by a significant reduction in the fluorescent signal when increasing amounts were added to the SYBR Green I-dsDNA complex. Our current work cannot distinguish between the two quenching mechanisms of these MILs as being spin-orbit coupling or excited-state electron transfer, however through the small overlap integral between

the absorption spectrum of each MIL and the emission spectrum of the SYBR Green I-dsDNA complex, it can be concluded that non-radiative Förster resonance energy transfer is not significant. Therefore, it can be concluded that these types of MILs are not recommended for direct use in fluorescence-based assays.

The Ni(II)-based MILs, $[Ni(BIm)_4^{2+}]2[Cl^-]$ and $[Ni(BnIm)_4^{2+}]2[Cl^-]$, quenched fluorescent signal equally, within experimental error. However, careful observation of the absorption spectra of the SYBR Green I-dsDNA complex with the $[Ni(BnIm)_4^{2+}]2[Cl^-]$ MIL revealed a possible static quenching component, thereby rendering the use of the $[Ni(BIm)_4^{2+}]2[Cl^-]$ MIL in fluorescence-based assays as a possibility. Based on the evaluation of these MILs with SYBR Green I-dsDNA as the fluorescent probe, it is recommended that caution be taken in using these MILs directly in fluorescence-based experiments. In PCR experiments in particular, customized PCR buffers containing metal chelators such as ethylenediaminetetraacetic acid (EDTA) can be designed to alleviate inhibition caused by the MILs if they are used in DNA extractions and directly added to the PCR buffer. This is similar to what was performed with previous generations of MILs which contained the metal in the anion.[15,25]

3.6. Acknowledgements

J. L. A. acknowledges funding from the Chemical Measurement and Imaging Program at the National Science Foundation (CHE-1709372).

3.7. References

(1) Yershov, G.; Barsky, V.; Belgovskiy, A.; Kirillov, E.; Kreindlin, E.; Ivanov, I.; Parinov, S.; Guschin, D.; Drobishev, A.; Dubiley, S.; et al. DNA Analysis and Diagnostics on Oligonucleotide Microchips. Proc. Natl. Acad. Sci. U. S. A. 1996, 93 (10), 4913–4918. https://doi.org/10.1073/pnas.93.10.4913.

(2) Evans, W. E.; Relling, M. V. Moving towards Individualized Medicine with Pharmacogenomics. Nature 2004, 429 (6990), 464–468. https://doi.org/10.1038/nature02626.

(3) Butler, J. M. The Future of Forensic DNA Analysis. Philos. Trans. R. Soc. B Biol. Sci. 2015, 370 (1674). https://doi.org/10.1098/rstb.2014.0252.

(4) Newman, M. E.; Parboosingh, J. S.; Bridge, P. J.; Ceri, H. Identification of Archaeological Animal Bone by PCR/DNA Analysis. J. Archaeol. Sci. 2002, 29 (1), 77–84. https://doi.org/10.1006/jasc.2001.0688.

(5) Auricchio, B.; Anniballi, F.; Fiore, A.; Skiby, J. E.; De Medici, D. Evaluation of DNA Extraction Methods Suitable for PCR-Based Detection and Genotyping of Clostridium Botulinum. Biosecurity and Bioterrorism 2013, 11 (1), 200–206. https://doi.org/10.1089/bsp.2012.0082.

(6) Nishi, K.; Isobe, S. I.; Zhu, Y.; Kiyama, R. Fluorescence-Based Bioassays for the Detection and Evaluation of Food Materials. Sensors (Switzerland) 2015, 15 (10), 25831–25867. https://doi.org/10.3390/s151025831.

(7) Green, M. R.; Sambrook, J. Molecular Cloning: A Laboratroy Manual, 4th ed.; Cold Springs Harbor Laboratory Press: Cold Springs Harbor, NY, USA, 2012.

(8) Tan, S. C.; Yiap, B. C. DNA, RNA, and Protein Extraction: The Past and The Present. J. Biomed. Biotechnol. 2009, 2009, 1–10. https://doi.org/10.1155/2009/574398.

(9) Lienhard, A.; Schäffer, S. Extracting the Invisible: Obtaining High Quality DNA Is a Challenging Task in Small Arthropods. PeerJ 2019, 7, 1–17. https://doi.org/10.7717/peerj.6753.

(10) Gumińska, N.; Płecha, M.; Walkiewicz, H.; Hałakuc, P.; Zakryś, B.; Milanowski, R. Culture Purification and DNA Extraction Procedures Suitable for Next-Generation Sequencing of Euglenids. J. Appl. Phycol. 2018, 30 (6), 3541–3549. https://doi.org/10.1007/s10811-018-1496-0.

(11) Wang, J. H.; Cheng, D. H.; Chen, X. W.; Du, Z.; Fang, Z. L. Direct Extraction of Double-Stranded DNA into Ionic Liquid 1-Butyl-3-Methylimidazolium Hexafluorophosphate and Its Quantification. Anal. Chem. 2007, 79 (2), 620–625. https://doi.org/10.1021/ac061145c.

(12) Li, T.; Joshi, M. D.; Ronning, D. R.; Anderson, J. L. Ionic Liquids as Solvents for in Situ Dispersive Liquid-Liquid Microextraction of DNA. J. Chromatogr. A 2013, 1272, 8–14. https://doi.org/10.1016/j.chroma.2012.11.055.

(13) Clark, K. D.; Nacham, O.; Yu, H.; Li, T.; Yamsek, M. M.; Ronning, D. R.; Anderson, J. L. Extraction of DNA by Magnetic Ionic Liquids: Tunable Solvents for Rapid and Selective DNA Analysis. Anal. Chem. 2015, 87 (3), 1552–1559. https://doi.org/10.1021/ac504260t.

(14) Clark, K. D.; Sorensen, M.; Nacham, O.; Anderson, J. L. Preservation of DNA in Nuclease-Rich Samples Using Magnetic Ionic Liquids. RSC Adv. 2016, 6 (46), 39846–39851. https://doi.org/10.1039/c6ra05932e.

(15) Emaus, M. N.; Clark, K. D.; Hinners, P.; Anderson, J. L. Preconcentration of DNA Using Magnetic Ionic Liquids That Are Compatible with Real-Time PCR for Rapid Nucleic Acid Quantification. Anal. Bioanal. Chem. 2018, 4135–4144. https://doi.org/10.1007/s00216-018-1092-9.

(16) Clark, K. D.; Varona, M.; Anderson, J. L. Ion-Tagged Oligonucleotides Coupled with a Magnetic Liquid Support for the Sequence-Specific Capture of DNA. Angew. Chemie - Int. Ed. 2017, 56 (26), 7630–7633. https://doi.org/10.1002/anie.201703299.

(17) Marengo, A.; Cagliero, C.; Sgorbini, B.; Anderson, J. L.; Emaus, M. N.; Bicchi, C.; Bertea, C. M.; Rubiolo, P. Development of an Innovative and Sustainable One-Step Method for Rapid Plant DNA Isolation for Targeted PCR Using Magnetic Ionic Liquids. Plant Methods 2019, 15 (1), 1–11. https://doi.org/10.1186/s13007-019-0408-x.

(18) Clark, K. D.; Emaus, M. N.; Varona, M.; Bowers, A. N.; Anderson, J. L. Ionic Liquids: Solvents and Sorbents in Sample Preparation. J. Sep. Sci. 2018, 41 (1). https://doi.org/10.1002/jssc.201700864.

(19) Santos, E.; Albo, J.; Irabien, A. Magnetic Ionic Liquids: Synthesis, Properties and Applications. RSC Adv. 2014, 4 (75), 40008–40018. https://doi.org/10.1039/c4ra05156d.

(20) Clark, K. D.; Nacham, O.; Purslow, J. A.; Pierson, S. A.; Anderson, J. L. Magnetic Ionic Liquids in Analytical Chemistry: A Review. Anal. Chim. Acta 2016, 934, 9–21. https://doi.org/10.1016/j.aca.2016.06.011.

(21) Trujillo-Rodríguez, M. J.; Nan, H.; Varona, M.; Emaus, M. N.; Souza, I. D.; Anderson, J. L. Advances of Ionic Liquids in Analytical Chemistry. Anal. Chem. 2019, 91 (1), 505–531. https://doi.org/10.1021/acs.analchem.8b04710.

(22) Sajid, M. Magnetic Ionic Liquids in Analytical Sample Preparation: A Literature Review. TrAC - Trends Anal. Chem. 2019, 113, 210–223. https://doi.org/10.1016/j.trac.2019.02.007.

(23) Hallett, J. P.; Welton, T. Room-Temperature Ionic Liquids: Solvents for Synthesis and Catalysis. 2. Chem. Rev. 2011, 111 (5), 3508–3576. https://doi.org/10.1021/cr1003248.

(24) Bowers, A. N.; Trujillo-Rodríguez, M. J.; Farooq, M. Q.; Anderson, J. L. Extraction of DNA with Magnetic Ionic Liquids Using in Situ Dispersive Liquid – Liquid Microextraction. Anal. Bioanal. Chem. 2019. https://doi.org/https://doi.org/10.1007/s00216-019-02163-9.

(25) Clark, K. D.; Yamsek, M. M.; Nacham, O.; Anderson, J. L. Magnetic Ionic Liquids as PCR-Compatible Solvents for DNA Extraction from Biological Samples. Chem. Commun. 2015, 51 (94), 16771–16773. https://doi.org/10.1039/c5cc07253k.

(26) Santra, K.; Clark, K. D.; Maity, N.; Petrich, J. W.; Anderson, J. L. Exploiting Fluorescence Spectroscopy to Identify Magnetic Ionic Liquids Suitable for the Isolation of Oligonucleotides. J. Phys. Chem. B 2018, 122, 7747–7756. https://doi.org/10.1021/acs.jpcb.8b05580.

(27) Fleming, G. R. Chemical Applications of Ultrafast Spectroscopy; Oxford University Press: New York, NY, 1986.

(28) Lakowicz, J. R. Principles of Fluorescence Spectroscopy, 3rd ed.; Springer: New York, NY, 2006.

(29) Stern, O.; Volmer, M. No Title. Phys. Z. 1919, 20 (183).

(30) Varnes, A. W.; Dodson, R. B.; Wehry, E. L. Interactions of Transition-Metal Ions with Photoexcited States of Flavins. Fluorescence Quenching Studies. J. Am. Chem. Soc. 1972, 94 (3), 946–950. https://doi.org/10.1021/ja00758a037.

(31) Yue, Q.; Hou, Y.; Yue, S.; Du, K.; Shen, T.; Wang, L.; Xu, S.; Li, H.; Liu, J. Construction of an Off-on Fluorescence System Based on Carbon Dots for Trace Pyrophosphate Sensing. J. Fluoresc. 2015, 25 (3), 585–594. https://doi.org/10.1007/s10895-015-1538-9.

(32) Yao, C.; Anderson, J. L. Dispersive Liquid-Liquid Microextraction Using an in Situ Metathesis Reaction to Form an Ionic Liquid Extraction Phase for the Preconcentration of Aromatic Compounds from Water. Anal. Bioanal. Chem. 2009, 395 (5), 1491–1502. https://doi.org/10.1007/s00216-009-3078-0.

(33) Chand, D.; Farooq, M. Q.; Pathak, A. K.; Li, J.; Smith, E. A.; Anderson, J. L. Magnetic Ionic Liquids Based On Transition-Metal Complexes with N-Alkylimidazole Ligands. New J. Chem. 2019, 43, 20–23. https://doi.org/10.1039/C8NJ05176C.

(34) Fraiji, L. K.; Hayes, D. M.; Werner, T. C. Static and Dynamic Fluorescence Quenching Experiments for the Physical Chemistry Laboratory. J. Chem. Educ. 1992, 69 (5), 424. https://doi.org/10.1021/ed069p424.

(35) Lehrer, S. S. Solute Perturbation of Protein Fluorescence. The Quenching of the Tryptophyl Fluorescence of Model Compounds and of Lysozyme by Iodide Ion. Biochemistry 1971, 10 (17), 3254–3263. https://doi.org/10.1021/bi00793a015.

(36) Keizer, J. Nonlinear Fluorescence Quenching and the Origin of Positive Curvature in Stern-Volmer Plots. J. Am. Chem. Soc. 1983, 105 (6), 1494–1498. https://doi.org/10.1021/ja00344a013.

(37) Wang, Y. Q.; Zhang, H. M.; Zhang, G. C.; Tao, W. H.; Tang, S. H. Interaction of the Flavonoid Hesperidin with Bovine Serum Albumin: A Fluorescence Quenching Study. J. Lumin. 2007, 126 (1), 211–218. https://doi.org/10.1016/j.jlumin.2006.06.013.

(38) Xing, D.; Dorr, R.; Cunningham, R. P.; Scholes, C. P. Endonuclease III Interactions with DNA Substrates. 2. The DNA Repair Enzyme Endonuclease III Binds Differently to Intact DNA and to Apyrimidinic/Apurinic DNA Substrates As Shown by Tryptophan Fluorescence Quenching. Biochemistry 1995, 34 (8), 2537–2544. https://doi.org/10.1021/bi00008a018.

(39) Förster, T. . Transfer Mechanisms of Electronic Excitation Energy. Radiat. Res. Suppl. 1960, 2, 326–339.

(40) Hunter, C. A.; Sanders, J. K. M. The Nature of π-π Interactions. J. Am. Chem. Soc. 1990, 112 (14), 5525–5534. https://doi.org/10.1021/ja00170a016.

CHAPTER 4. GENERAL CONCLUSIONS

This thesis summarizes the application of a new generation of MILs containing paramagnetic cations for the extraction of dsDNA. Additionally, the fluorescence quenching effects of these MILs were evaluated using the SYBR Green I-dsDNA complex as the fluorescent probe. The MILs applied in these studies possess many advantageous properties such as facile and inexpensive to prepare, low viscosity of the MIL solution, *in situ* formation of the hydrophobic MIL during extractions and paramagnetic nature allowing for magnetic manipulation.

Chapter 2 describes the extraction of dsDNA with MILs using *in situ* DLLME coupled to indirect detection using HPLC-DAD or fluorescence spectroscopy. A comparison to conventional MIL-DLLME using the water-immiscible MIL analogs was performed to demonstrate the beneficial effect of using the *in situ* approach. Higher extraction efficiencies were obtained using the *in situ* MIL-DLLME method compared to conventional MIL-DLLME. Extraction efficiencies were also higher using this generation of MILs compared to a MIL used in previous DNA extractions, $[P_{66614}^{+}][Ni(II)(hfacac)_3^{-}]$. In general, the developed *in situ* MIL-DLLME method was also faster than other reported methods, with an extraction time of only 3 min.

Chapter 3 investigates the fluorescence quenching effects of this new generation of MILs, using a common DNA binding dye, SYBR Green I, bound with dsDNA as the fluorophore complex. Metal salts and an IL were used as controls to elucidate the origin in the MIL structure responsible for fluorescence quenching. Fitting the data to Stern-Volmer models revealed the presence of two populations of fluorophores, with different fractions of accessibility to the quencher molecules, as provided by the SYBR Green I dye intercalated within the dsDNA. The

ability of the MILs to efficiently quench the fluorescence signal was found to be through either spin-orbit coupling or excited-state electron transfer, as there was little overlap between the absorbance spectrum of each of the metal salts and MILs and the fluorescence emission spectrum of the SYBR Green I-dsDNA complex. Through evaluation of this data, the direct use of these MILs in fluorescence-based assays is not recommended, as they are shown to be strong quenchers. However, future work could test this claim in specific systems and design appropriate buffers through the addition of metal chelators or other reagents to potentially mitigate the quenching caused by these MILs.

APPENDIX A. SUPPLEMENTAL INFORMATION ACCOMPANYING CHAPTER 2

Table A1. Volumes of MIL and $LiNTf_2$ stock solutions needed to produce a droplet using the *in situ* DLLME method for extraction of DNA.

MIL applied for *in situ* DLLME	**Volume of the MIL stock solution added (µL)[a]**	**Volume of the $LiNTf_2$ stock solution added (µL)[b]**	**Molar ratio of MIL:$LiNTf_2$**
$[Ni(BIm)_4^{2+}]2[Cl^-]$	638	23	1:2
$[Ni(BnIm)_4^{2+}]2[Cl^-]$	691	23	1:2.8
$[Mn(BIm)_4^{2+}]2[Cl^-]$	800	23	1:2.5
$[Co(BIm)_4^{2+}]2[Cl^-]$	805	29	1:2.5

[a] The concentration of the MIL stock solution was 20 $mg \cdot mL^{-1}$ except for the $[Ni(BIm)_4^{2+}]2[Cl^-]$ MIL, which had a concentration of 25 $mg \cdot mL^{-1}$.

[b] The concentration of the $LiNTf_2$ stock solution was 600 $mg \cdot mL^{-1}$.

Table A2. Amounts of MIL required for the conventional DLLME method for extraction of DNA.

MIL applied for Conventional DLLME	**Amount of MIL added (µmol)[a]**
$[Ni(BIm)_4^{2+}]2[NTf_2^-]$	21
$[Ni(BnIm)_4^{2+}]2[NTf_2^-]$	18
$[Mn(BIm)_4^{2+}]2[NTf_2^-]$	21
$[Co(BIm)_4^{2+}]2[NTf_2^-]$	21
$[Mn(OIm)_4^{2+}][NTf_2^-]$	16
$[P_{66614}^+][Ni(II)(hfacac)_3^-]$	15

[a] Corresponds to 18 mg of MIL.

Table A3. Comparison of the extraction efficiency of DNA by the MILs using HPLC-DAD and fluorescence emission measurements at a 95% confidence level.

MIL	Fisher test				Student's t-test			
	F_o[a]	F_c[b]	Result		t_o[c]	t_c[d]	Result	
$[Ni(BIm)_4^{2+}]2[Cl^-]$	5.942	5.050	$F_o > F_c$	Unequal variances	1.749	2.365	$t_o < t_c$	Equal methods
$[Ni(BIm)_4^{2+}]2[NTf_2^-]$	8.820	19.00	$F_o < F_c$	Equal variances	0.5710	2.776	$t_o < t_c$	Equal methods
$[Ni(BnIm)_4^{2+}]2[NTf_2^-]$	25.18	19.00	$F_o > F_c$	Unequal variances	1.413	4.303	$t_o < t_c$	Equal methods
$[P_{66614}^+][Ni(II)(hfacac)_3^-]$	3.296	19.00	$F_o < F_c$	Equal variances	0.1104	2.776	$t_o < t_c$	Equal methods

[a] Observed value of the Fisher test.

[b] Critical value of the Fisher test at a 95% confidence level [19].

[c] Observed value of the Student's t-test.

[d] Critical value of the Student's t-test at a 95% confidence level [19].

[1] D.C. Harris, Quantitative Chemical Analysis, 8th ed., W. H. Freeman and Company, New York, NY, 2010.

Table A4. Amount of MIL remaining in the aqueous phase after the *in situ* DLLME method.

MIL applied for *in situ* DLLME	**Concentration of the MIL in the aqueous phase after extraction, C_{aq} (mM) (n = 3)**	**Concentration of the MIL used in the extraction, C_o (mM)**	**Percentage of the MIL in the aqueous phase after extraction, S_{MIL} (%)**
$[Ni(BIm)_4^{2+}]2[Cl^-]$	7.0 ± 1.3	11.9	58.8
$[Ni(BnIm)_4^{2+}]2[Cl^-]$	4.0 ± 0.8	8.57	46.7
$[Mn(BIm)_4^{2+}]2[Cl^-]$	2.9 ± 0.8	12.0	24.2
$[Co(BIm)_4^{2+}]2[Cl^-]$	4.7 ± 0.7	12.1	38.8

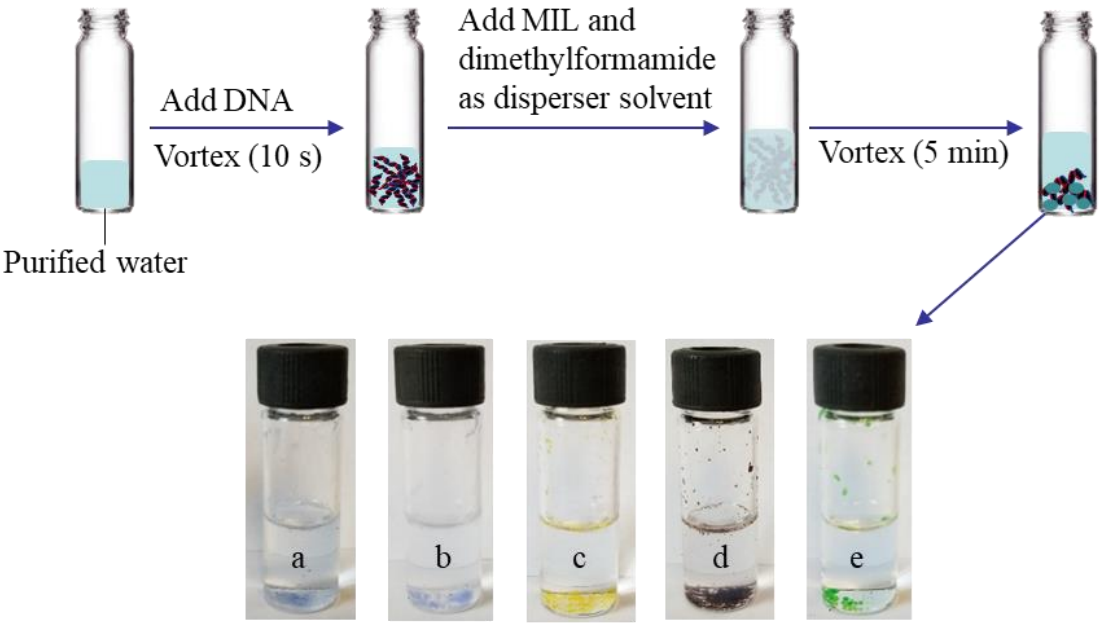

[a] $[Ni(BIm)_4^{2+}]2[NTf_2^-]$
[b] $[Ni(BnIm)_4^{2+}]2[NTf_2^-]$
[c] $[Mn(BIm)_4^{2+}]2[NTf_2^-]$
[d] $[Co(BIm)_4^{2+}]2[NTf_2^-]$
[e] $[P_{66614}^+][Ni(II)(hfacac)_3^-]$

Figure A1. Scheme for the conventional DLLME method using MILs for the extraction of DNA.

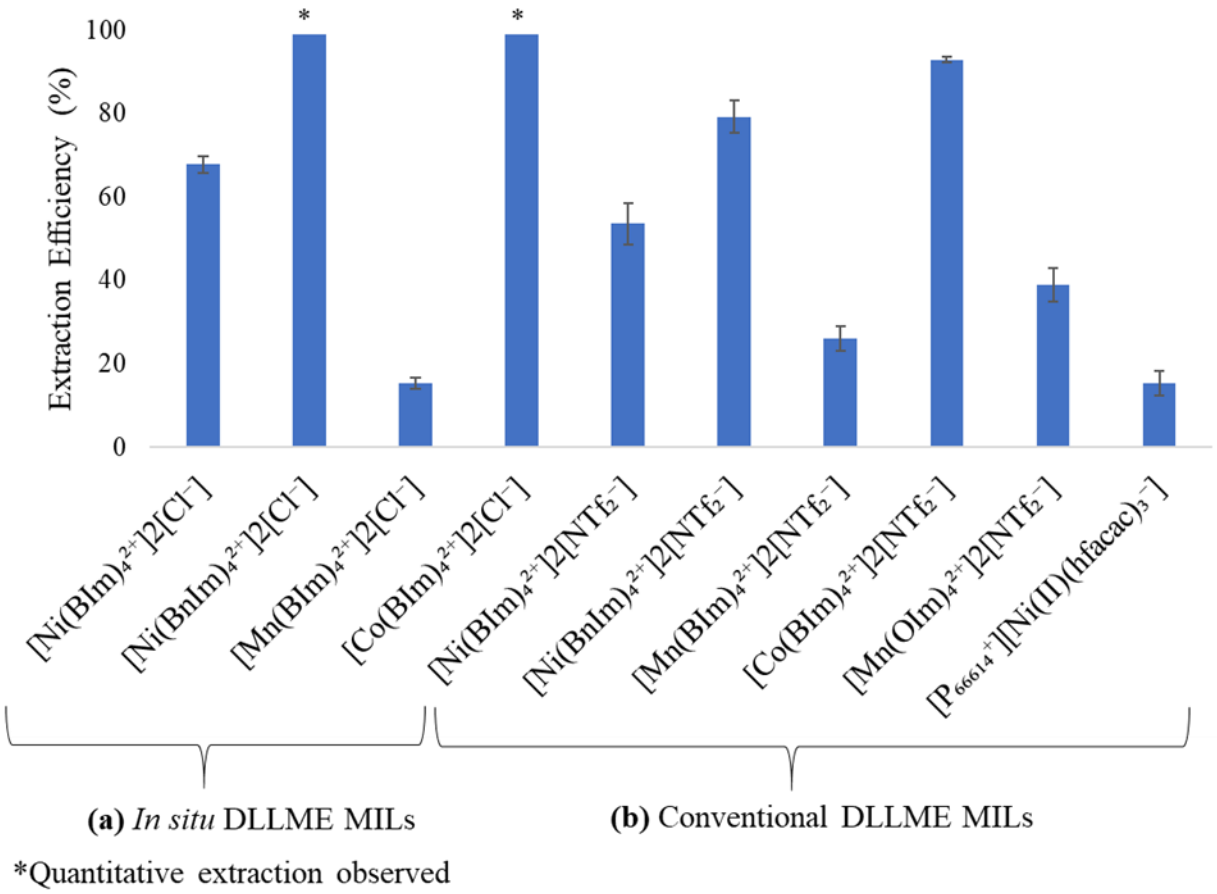

Figure A2. Extraction efficiencies (% EF) of ~20 kbp stDNA by each of the MILs using **(a)** MIL-based *in situ* DLLME or **(b)** conventional MIL-DLLME and HPLC-DAD detection. Experimental conditions (n = 3): 2 nM DNA, 2 mL total extraction volume, 15-24 µmol MIL, 300 µL dimethylformamide dispersive solvent, 3 min vortex at 2100 rpm. Note: For *in situ* DLLME, a range of 1:1.5 to 1:2.8 molar ratio of MIL:$[Li^+][NTf_2^-]$ was used, depending on the MIL. For the $[P_{66614}^+][Ni(II)(hfacac)_3^-]$ MIL, no dispersive solvent was used.

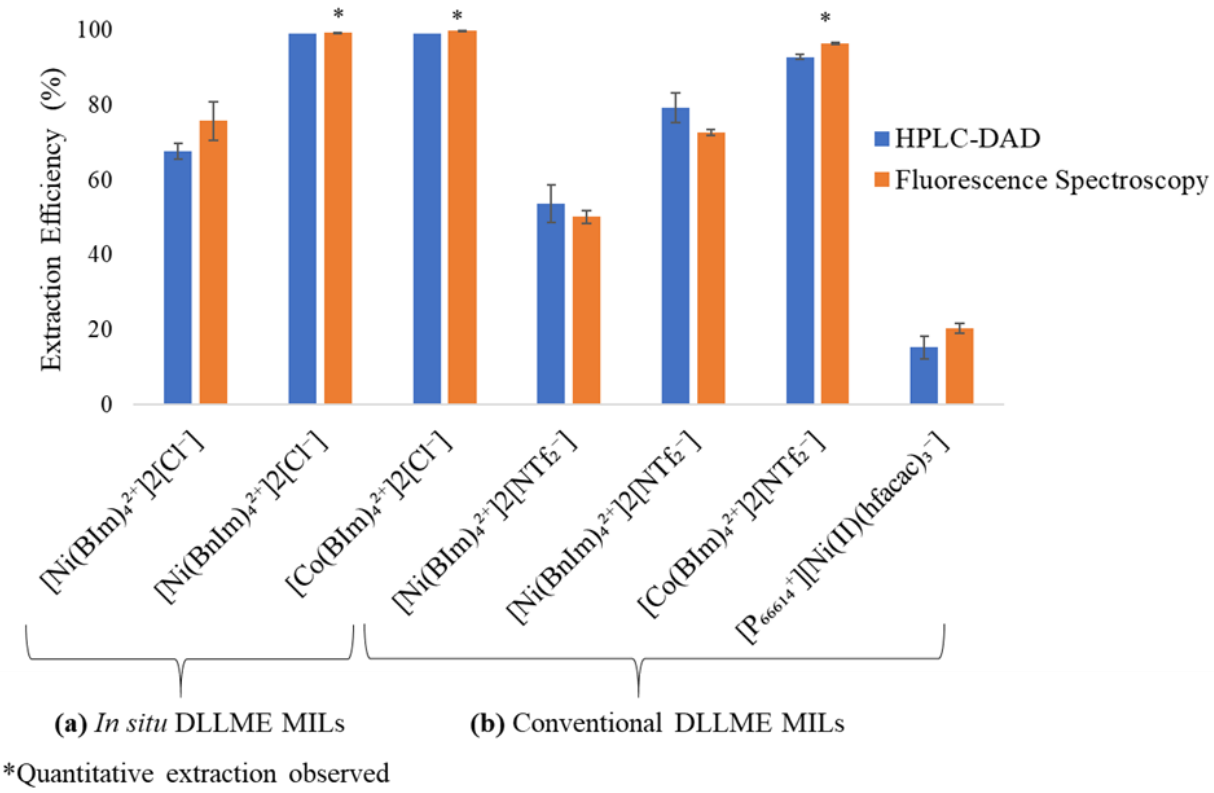

Figure A3. Comparison of extraction efficiencies (% EF) obtained using HPLC-DAD (blue) and fluorescence emission spectroscopy detection (orange). ~20 kbp stDNA was extracted by each of the MILs using **(a)** MIL-based *in situ* DLLME or **(b)** conventional MIL-DLLME and HPLC-DAD detection. Experimental conditions (n = 3): 2 nM DNA, 2 mL total extraction volume, 15-24 µmol MIL, 300 µL dimethylformamide dispersive solvent, 3 min vortex at 2100 rpm. Note: For *in situ* DLLME, a range of 1:1.5 to 1:2.8 molar ratio of MIL:$[Li^+][NTf_2^-]$ was used, depending on the MIL. For the $[P_{66614}^+][Ni(II)(hfacac)_3^-]$ MIL, no dispersive solvent was used.

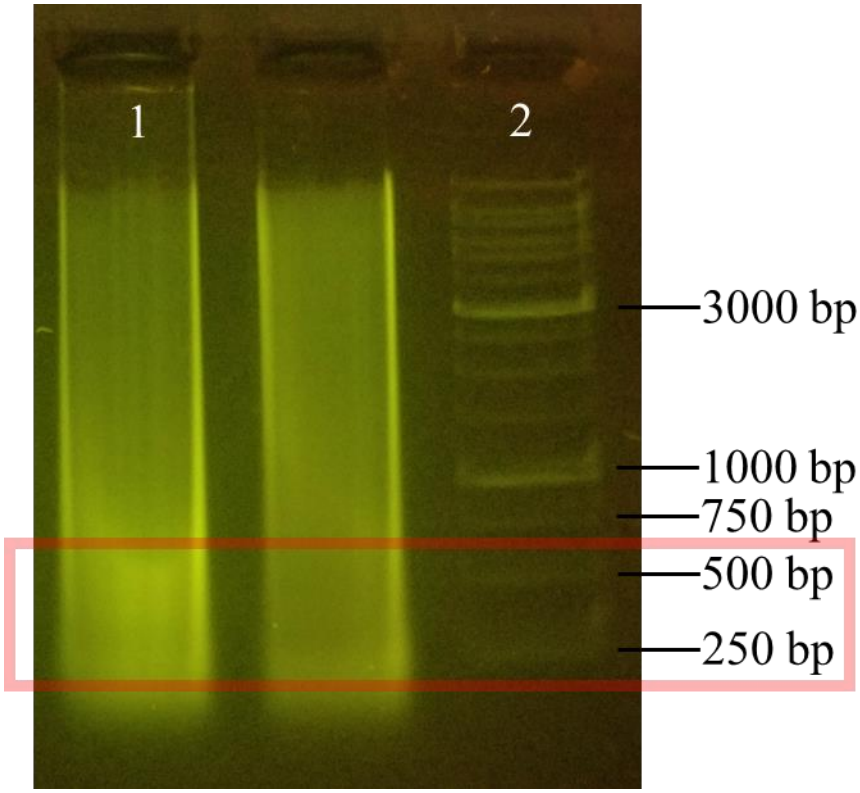

Figure A4. Agarose gel (1% w/v) electrophoresis separation confirming the size of the sheared salmon testes DNA (stDNA) fragments (lane 1) compared to a 1 kb DNA ladder (lane 2). stDNA was sheared for 60 cycles (1 cycle: 30 s on and 30 s off) through sonication in an ice bath.

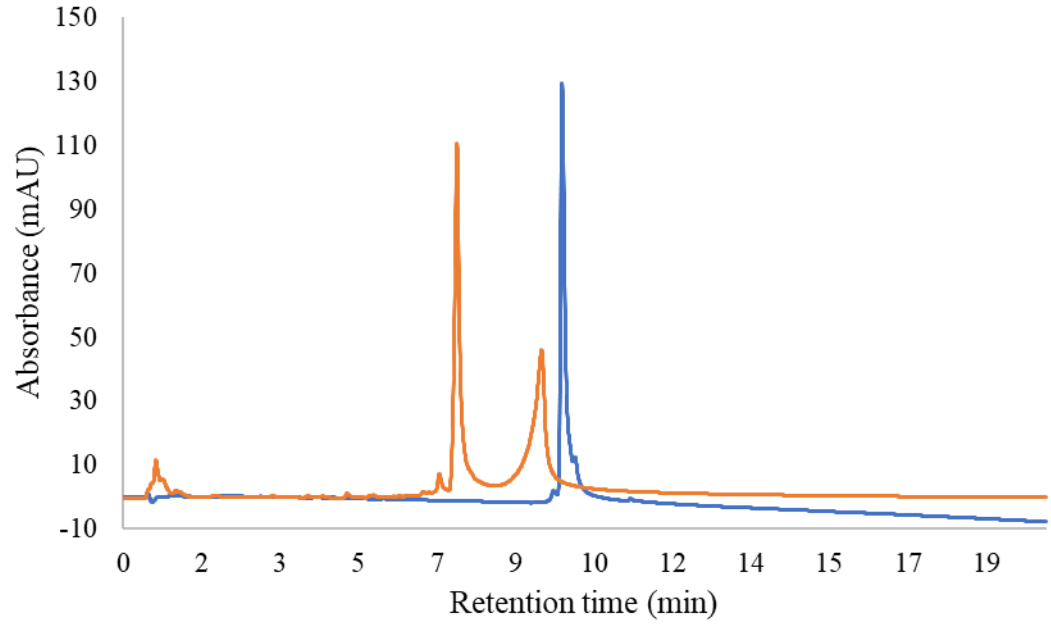

(a)

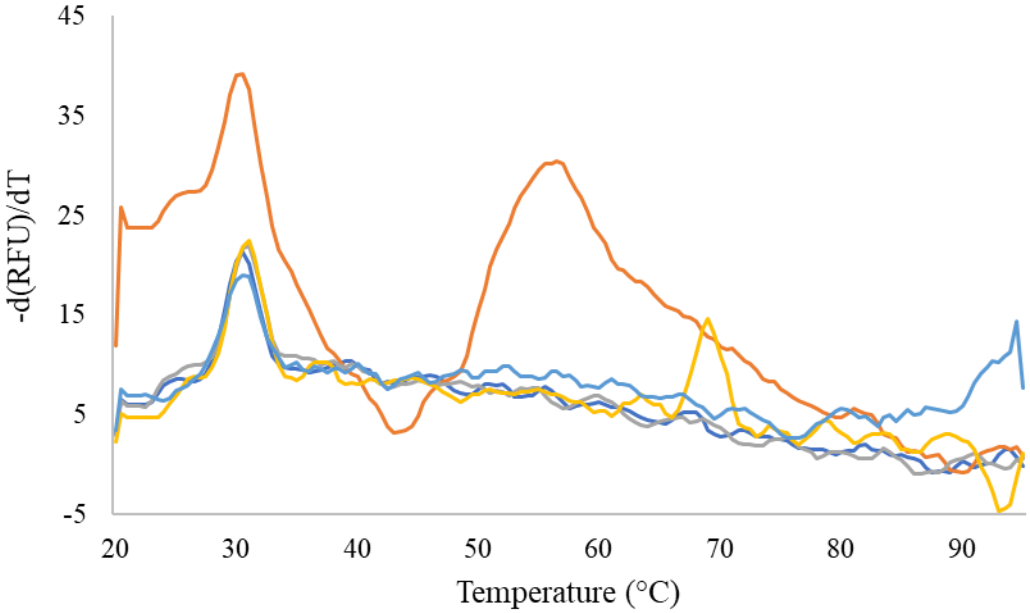

(b)

Figure A5. Confirmation of the annealed 20 bp DNA sequence; **(a)** Chromatographic overlay after HPLC-DAD detection of a 2 nM standard of the annealed 20 bp DNA (blue) and both complementary 20-mer DNA oligonucleotides that have not undergone the annealing process (orange). **(b)** Melt curve of annealed 20 bp DNA (orange), oligo 1 only (gray), oligo 2 only (yellow), both oligos not annealed (light blue) and a negative control (dark blue). Melting temperature, T_m (IDT Specification Sheet; 50 mM NaCl) = 58.0 °C, T_m (experimental; 100 mM NaCl) = 56.50 °C.

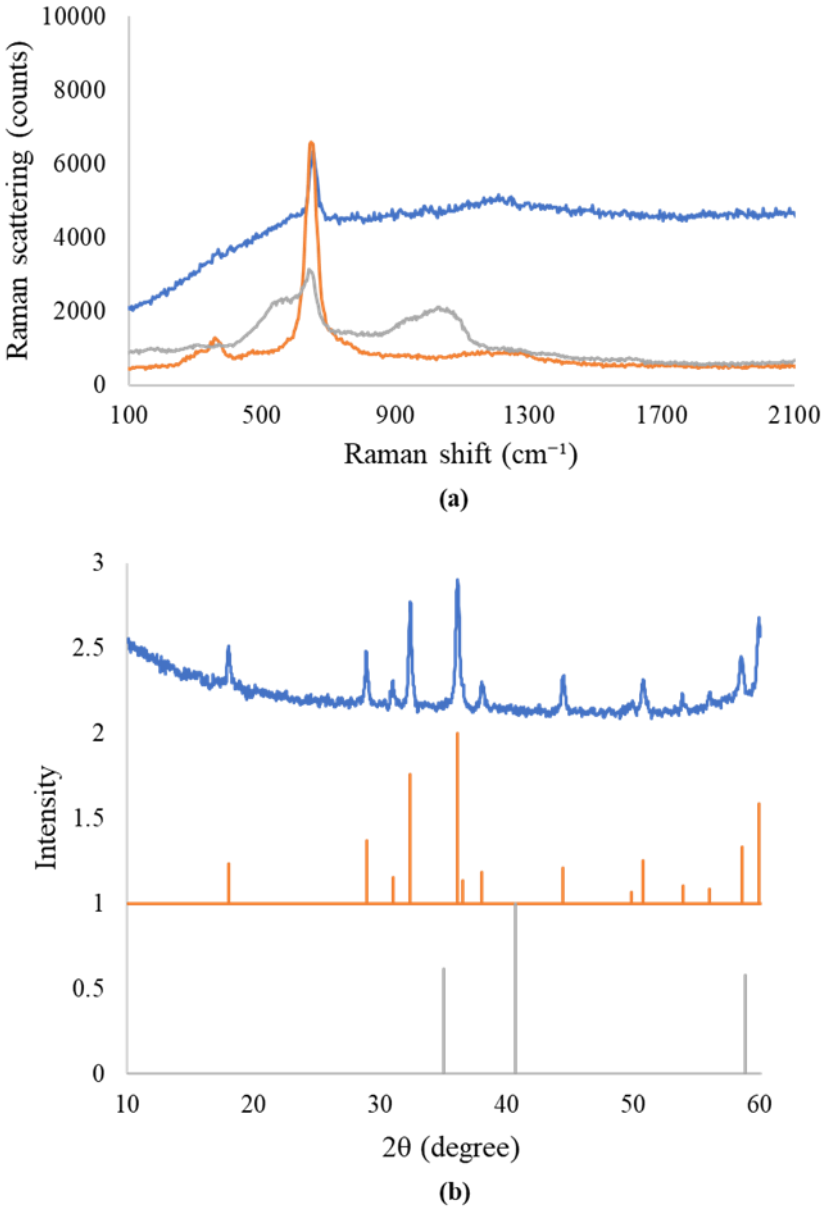

Figure A6. **(a)** Raman spectrum of the $[Mn(BIm)_4^{2+}]2[Cl^-]$ MIL precipitate (blue), manganese(II) oxide (MnO; gray) and manganese(II,III) oxide (Mn_3O_4; orange). The peak at 650 cm^{-1} is related with Mn-O vibrations. **(b)** X-ray diffraction pattern of the $[Mn(BIm)_4^{2+}]2[Cl^-]$ MIL precipitate (blue), MnO (gray) and Mn_3O_4 (orange).

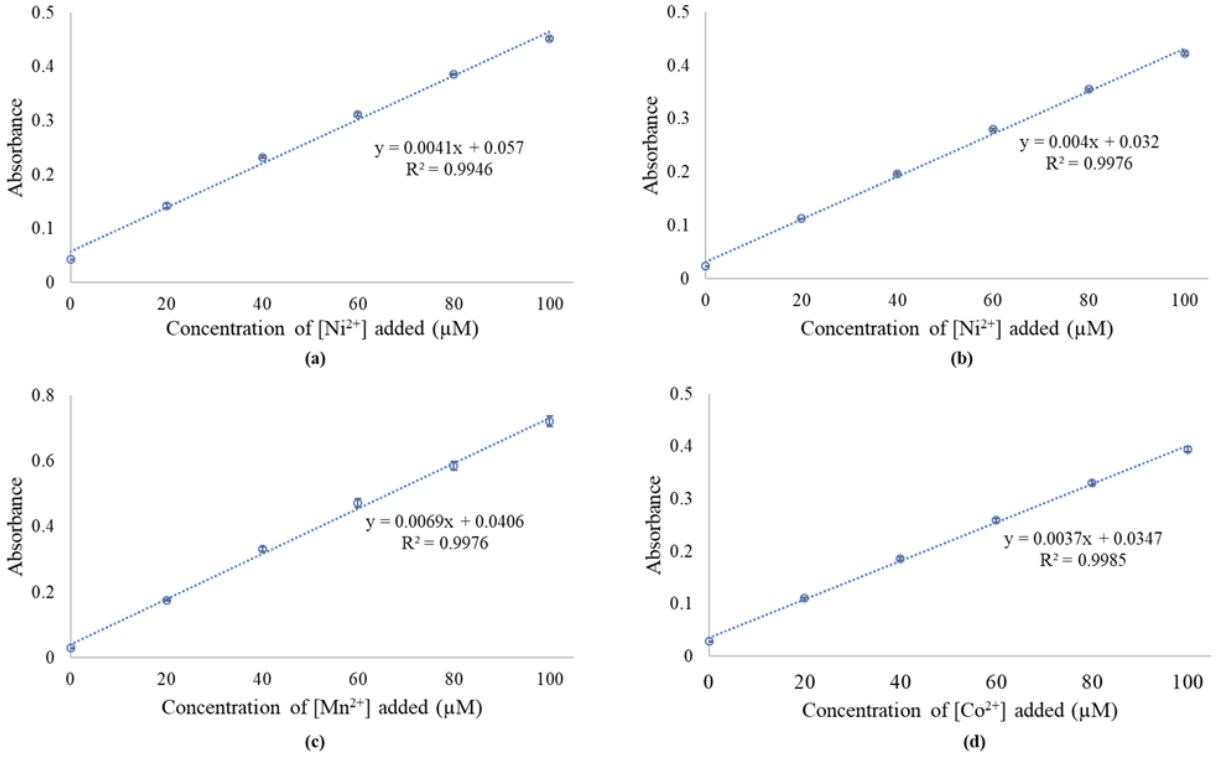

Figure A7. Standard addition plots for the determination of the metal concentration in the aqueous phase after *in situ* DLLME using flame atomic absorption spectroscopy. **(a)** $[Ni(BIm)_4^{2+}]2[Cl^-]$ MIL, **(b)** $[Ni(BnIm)_4^{2+}]2[Cl^-]$ MIL, **(c)** $[Mn(BIm)_4^{2+}]2[Cl^-]$ MIL, **(d)** $[Co(BIm)_4^{2+}]2[Cl^-]$ MIL.

APPENDIX B. SUPPLEMENTAL INFORMATION ACCOMPANYING CHAPTER 3

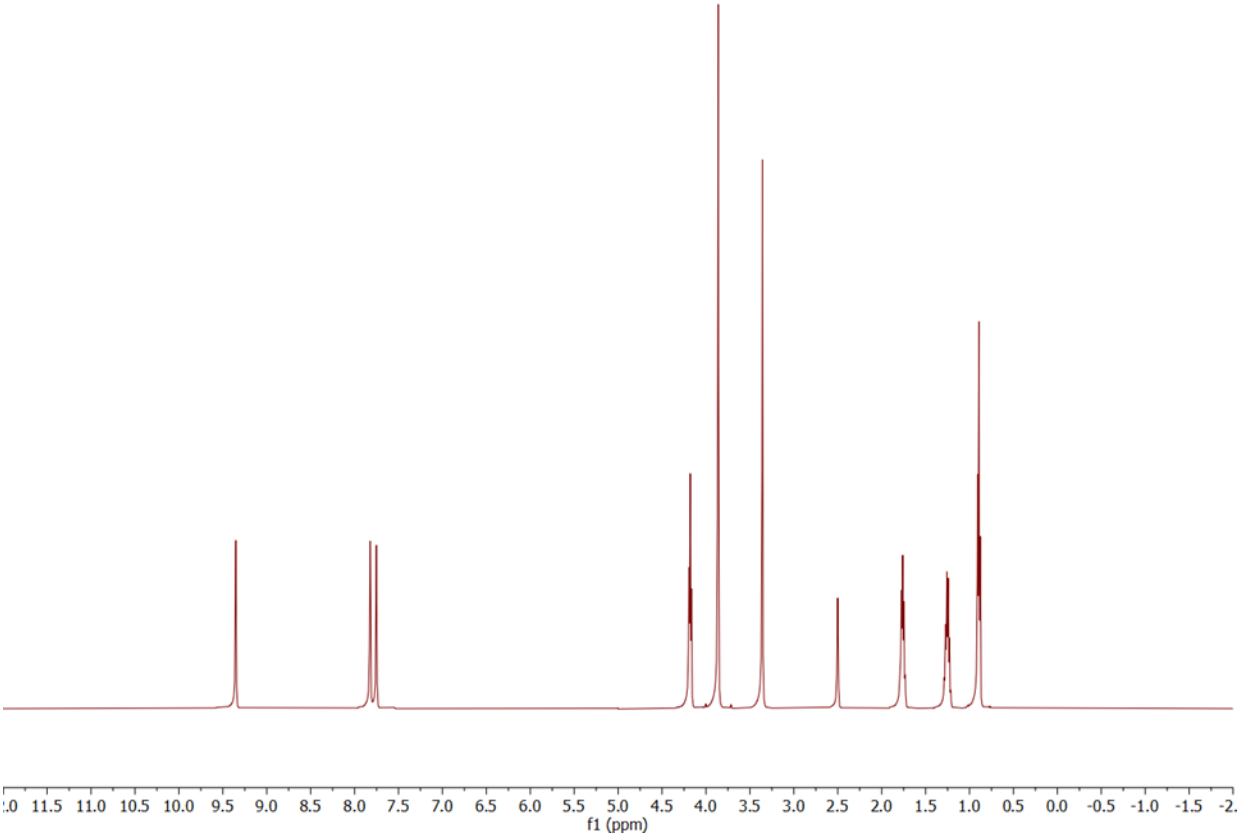

Figure B1. ^{1}H NMR spectrum of [BMIm^{+}][Cl^{-}]: ^{1}H NMR (500 MHz, DMSO-d_6) δ 9.35 (s, 1H), 7.82 (t, J = 1.6 Hz, 1H), 7.75 (t, J = 1.7 Hz, 1H), 4.18 (t, J = 7.1 Hz, 2H), 3.86 (s, 3H), 1.81-1.71 (m, 2H), 1.31-1.21 (m, 2H), 0.93-0.86 (m, 3H).

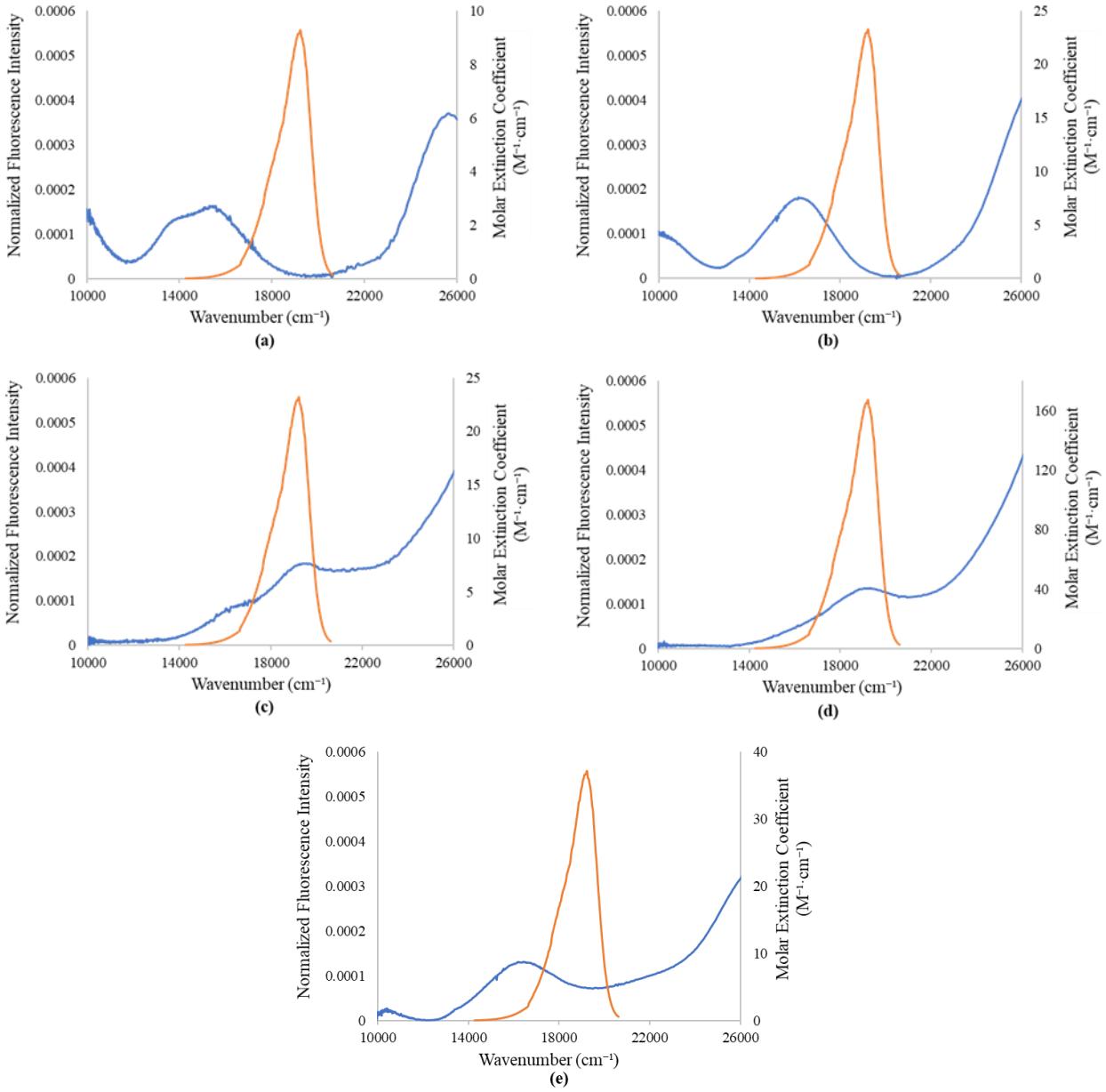

Figure B2. Fluorescence emission spectrum of SYBR green I-DNA (orange) and absorbance spectrum (blue) of (a) $NiCl_2$, (b) $[Ni(BIm)_4^{2+}]2[Cl^-]$, (c) $CoCl_2$, (d) $[Co(BIm)_4^{2+}]2[Cl^-]$ and (e) $[Ni(BnIm)_4^{2+}]2[Cl^-]$ with unit area on the wavenumber scale. The Förster overlap integral of the fluorescence emission spectrum and absorbance spectrum is required for the calculation of Förster critical distance *(R_0)*, the critical transfer distance between the fluorescent donor and acceptor.

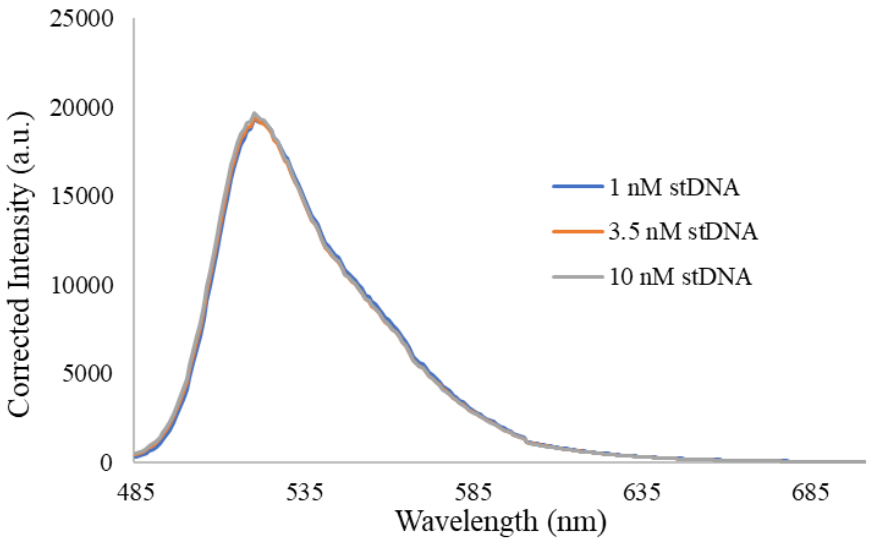

Figure B3. Fluorescence emission spectra of SYBR Green I-DNA complex, λ_{ex} = 475 nm. Intensities are corrected for the absorption at the wavelength of excitation. 1.96 µM SYBR Green I dye was used in all cases with with 1 nM (blue), 3.5 nM (orange) and 10 nM (gray) of stDNA.

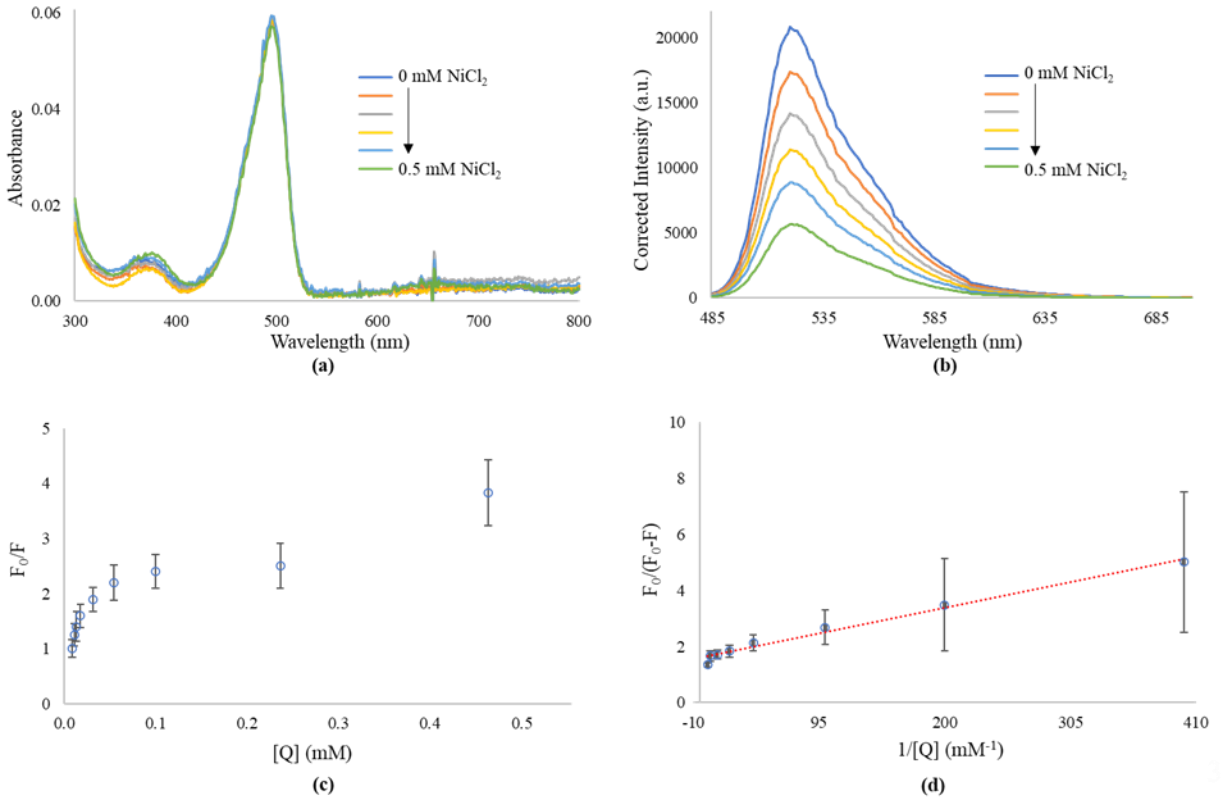

Figure B4. Fluorescence quenching of the SYBR Green I-dsDNA complex as a function of $NiCl_2$ concentration. **(a)** Absorption spectra. **(b)** Fluorescence emission spectra, λ_{ex} = 475 nm. Intensities were corrected for the absorption at the wavelength of excitation. **(c)** Steady-state Stern-Volmer plot of the integrate fluorescence intensity ratio (F_0/F) as a function of quencher concentration. **(d)** Steady-state modified Stern-Volmer plot of the integrated fluorescence intensity ratio ($F_0/(F_0-F)$) and as a function of $1/[Q]$.

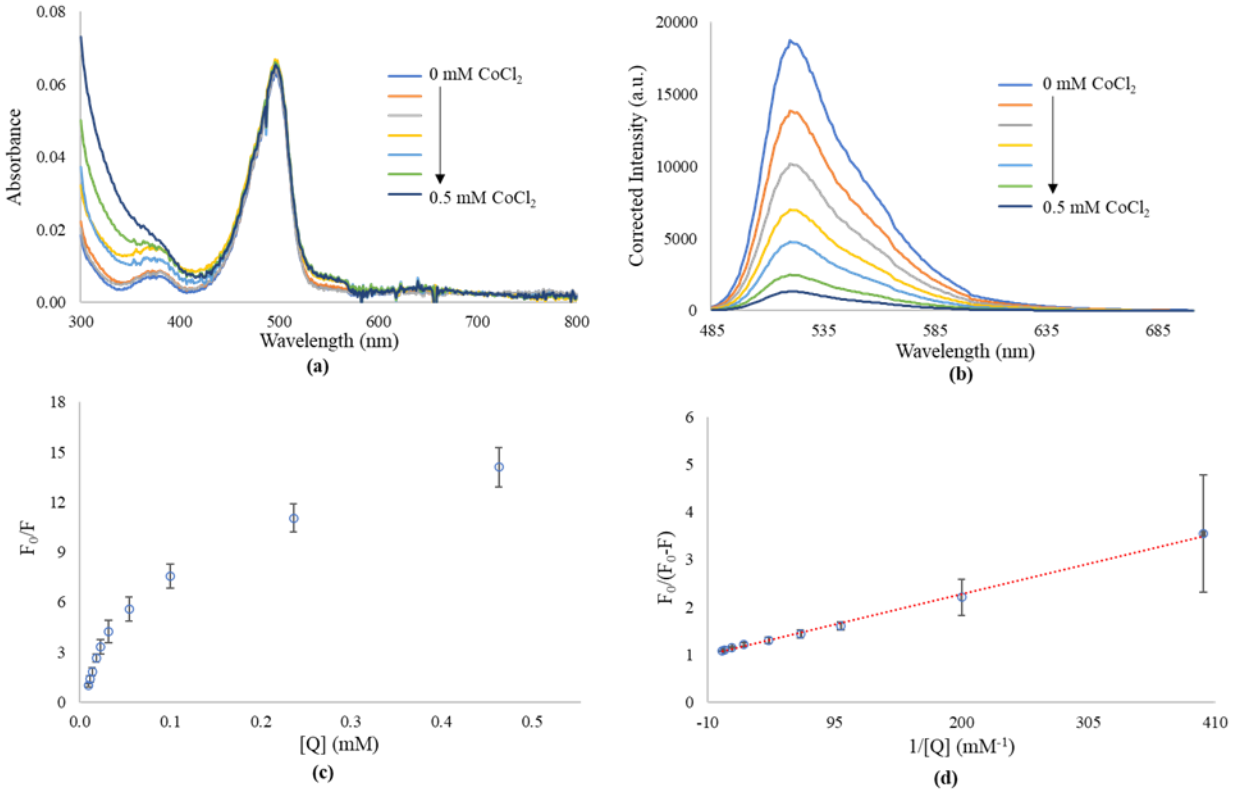

Figure B5. Fluorescence quenching of the SYBR Green I-dsDNA complex as a function of $CoCl_2$ concentration. **(a)** Absorption spectra. **(b)** Fluorescence emission spectra, λ_{ex} = 475 nm. Intensities were corrected for the absorption at the wavelength of excitation. **(c)** Steady-state Stern-Volmer plot of the integrate fluorescence intensity ratio (F_0/F) as a function of quencher concentration. **(d)** Steady-state modified Stern-Volmer plot of the integrated fluorescence intensity ratio ($F_0/(F_0-F)$) and as a function of $1/[Q]$

Table B1. Comparison of the integrated fluorescence intensities of the corrected emission spectra for the amount of dsDNA added to 1.96 µM SYBR Green I dye.

Amount of dsDNA compared to 1 nM dsDNA (nM)	Fisher test				Student's t-test			
	F_o[a]	F_c[b]	Result		t_o[c]	t_c[d]	Result	
3.5	1.048	19.00	$F_o < F_c$	Equal variances	0.533	2.776	$t_o < t_c$	Equal intensity
10	0.538	0.053	$F_o > F_c$	Unequal variances	2.113	2.776	$t_o < t_c$	Equal intensity

[a] Observed value of the Fisher test.

[b] Critical value of the Fisher test at a 95% confidence level.[19]

[c] Observed value of the Student's t-test.

[d] Critical value of the Student's t-test at a 95% confidence level [19].

[1]D.C. Harris, Quantitative Chemical Analysis, 8th ed., W. H. Freeman and Company, New York, NY, 2010.